

**LIDAR REMOTE SENSING DATA COLLECTION
DEPARTMENT OF GEOLOGY AND MINERAL INDUSTRIES
SOUTH COAST, OREGON**

MAY 8, 2009

Submitted to:

Department of Geology and Mineral Industries
800 NE Oregon Street, Suite 965
Portland, OR 97232



Submitted by:

Watershed Sciences
529 SW 3rd Avenue, Suite 300
Portland, OR 97204



LIDAR REMOTE SENSING DATA COLLECTION: DOGAMI, SOUTH COAST STUDY AREA

TABLE OF CONTENTS

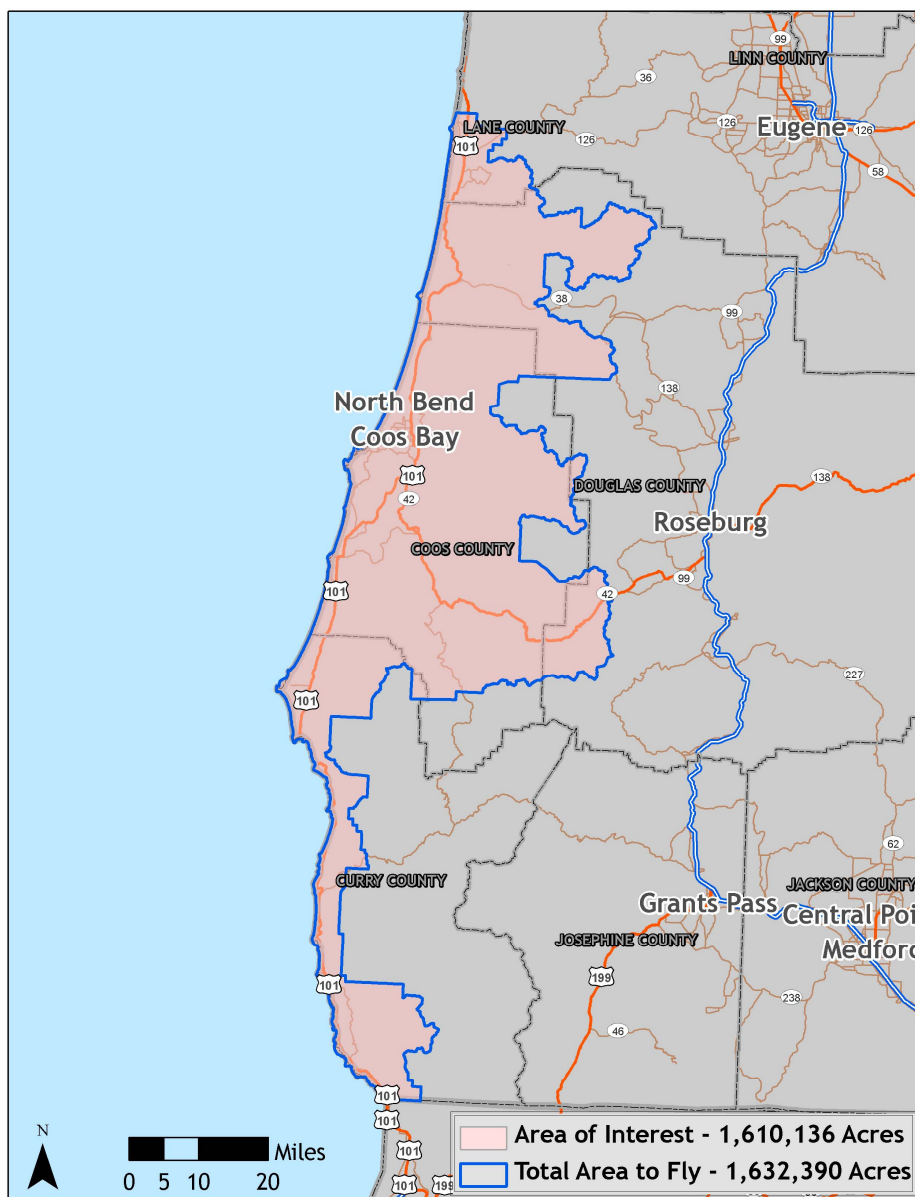
1. Overview	1
1.1 Study Area (South Coast)	1
1.2 Area Delivered to Date	2
1.3 Acquisition and Ground Survey	4
2. Accuracy.....	13
2.1 Relative Accuracy.....	13
2.2 Absolute Accuracy.....	13
3. Data Density/Resolution.....	15
3.1 Density Statistics.....	15
3.2 Data Density/Resolution per Delivery	19
3.2.1 Delivery 1	19
3.2.2 Delivery 2	20
3.2.3 Delivery 3	22
3.2.4 Delivery 4.....	23
4. Selected Imagery	25

1. Overview

1.1 Study Area (South Coast)

Watershed Sciences, Inc. has collected Light Detection and Ranging (LiDAR) data of the South Coast study area for the Oregon Department of Geology and Mineral Industries (DOGAMI). The Area of Interest (AOI) covers portions of four counties in southwest Oregon. The requested LiDAR area totals ~1,610,136 acres; the map below shows the Total Area to be Flown (TAF), covering ~1,632,390 acres. The TAF acreage is greater than the original AOI acreage due to buffering and flight planning optimization. This report will be amended to reflect new data and cumulative statistics for the overall LiDAR survey. DOGAMI data are *delivered* in OGIC(HARN): Projection: Oregon Statewide Lambert Conformal Conic; horizontal and vertical datums: NAD83 (HARN)/NAVD88(Geoid03); Units: International Feet.

Figure 1.1. DOGAMI South Coast study area.



1.2 Area Delivered to Date

Table 1.1. Total delivered acreage to date.

DOGAMI Southern Oregon Coast				
	Delivery Date	Acquisition Date	AOI Acres	TAF Acres
Delivery 1	September 3, 2008	May 3 - June 26, 2008	46,568	47,798
Delivery 2	October 2, 2008	May 3 - June 26, 2008	86,505	88,789
Delivery 3	October 16, 2008	May 3 - June 26, 2008	68,913	71,791
Delivery 4	November 21, 2008	June 12 - June 29, 2008	111,851	113,638
Delivery 5	January 19, 2009	June 12 - June 29, 2008	113,350	113,794
Delivery 6	April 15, 2009	June 15 - August 9, 2008	221,939	222,692
Delivery 7	April 15, 2009	June 15 - August 9, 2008	133,226	134,276
Delivery 8a	April 15, 2009	June 15 - August 9, 2008	91,453	93,631
Delivery 8b	May 8, 2009	June 8 - Oct. 19, 2008	47,388	48,275
Delivery 9	May 8, 2009	June 15 - Oct. 19, 2008	139,023	139,024
Delivery 10	May 8, 2009	June 29 - Sept. 28, 2008	143,891	145,854
		Total	1,204,107	1,219,562

Figure 1.2. DOGAMI southern Oregon coast study area, illustrating the delivered portion of the TAF.

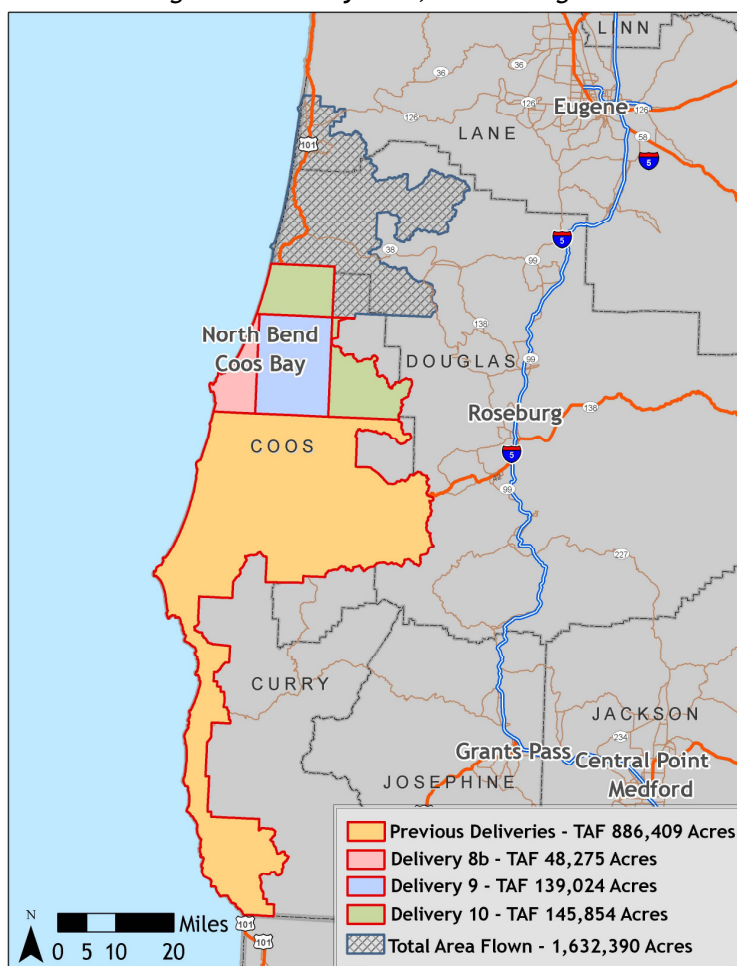
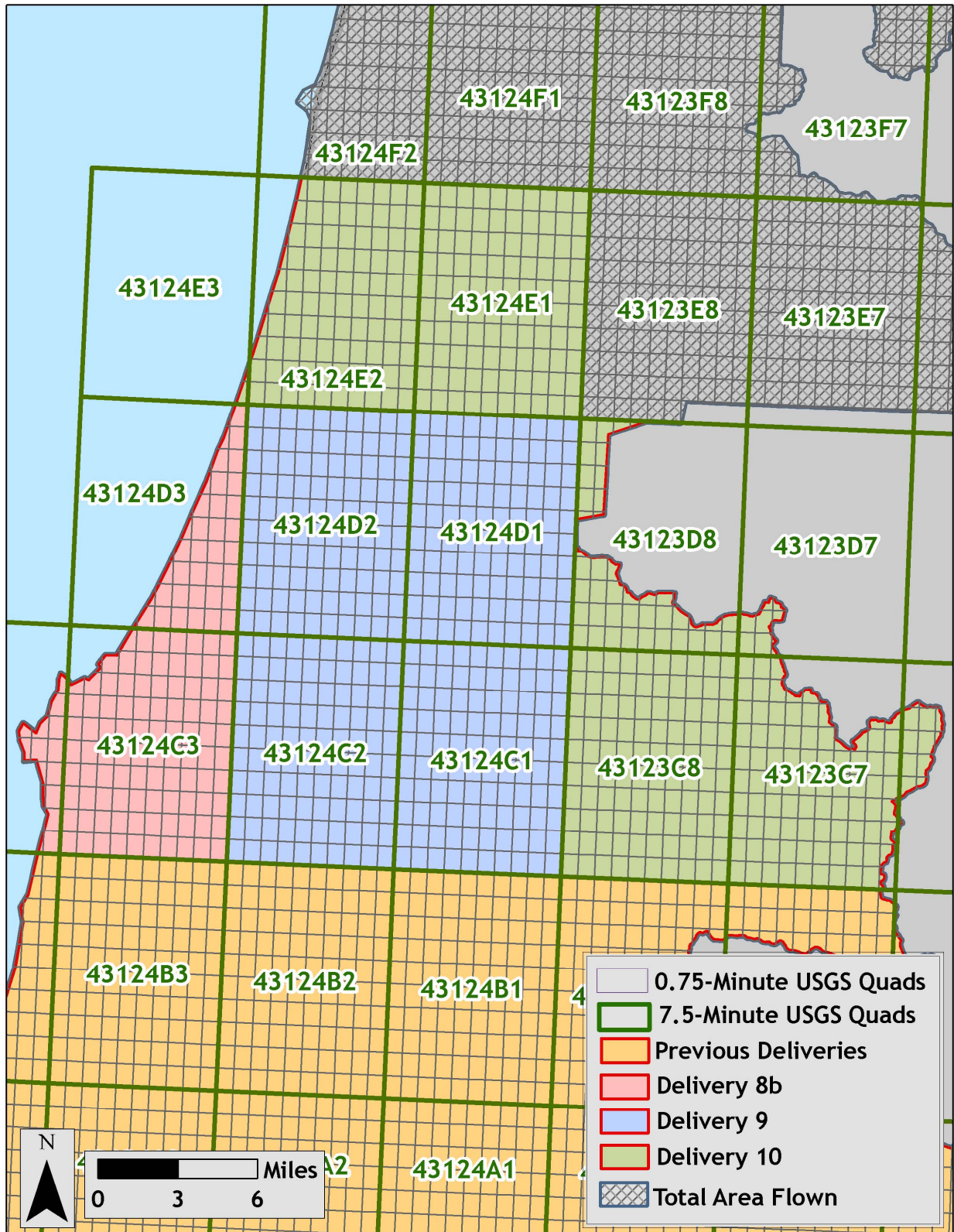


Figure 1.3. South Coast study area, illustrating the delivered 7.5 and 0.75-minute USGS quads.



1.3 Acquisition and Ground Survey

LiDAR acquisition for all data occurred from April 27, 2008 to April 5, 2009 for the South Coast study area.

Figure 1.4. Actual flightlines for the South Coast study area illustrating the dates flown (based on GPS week).

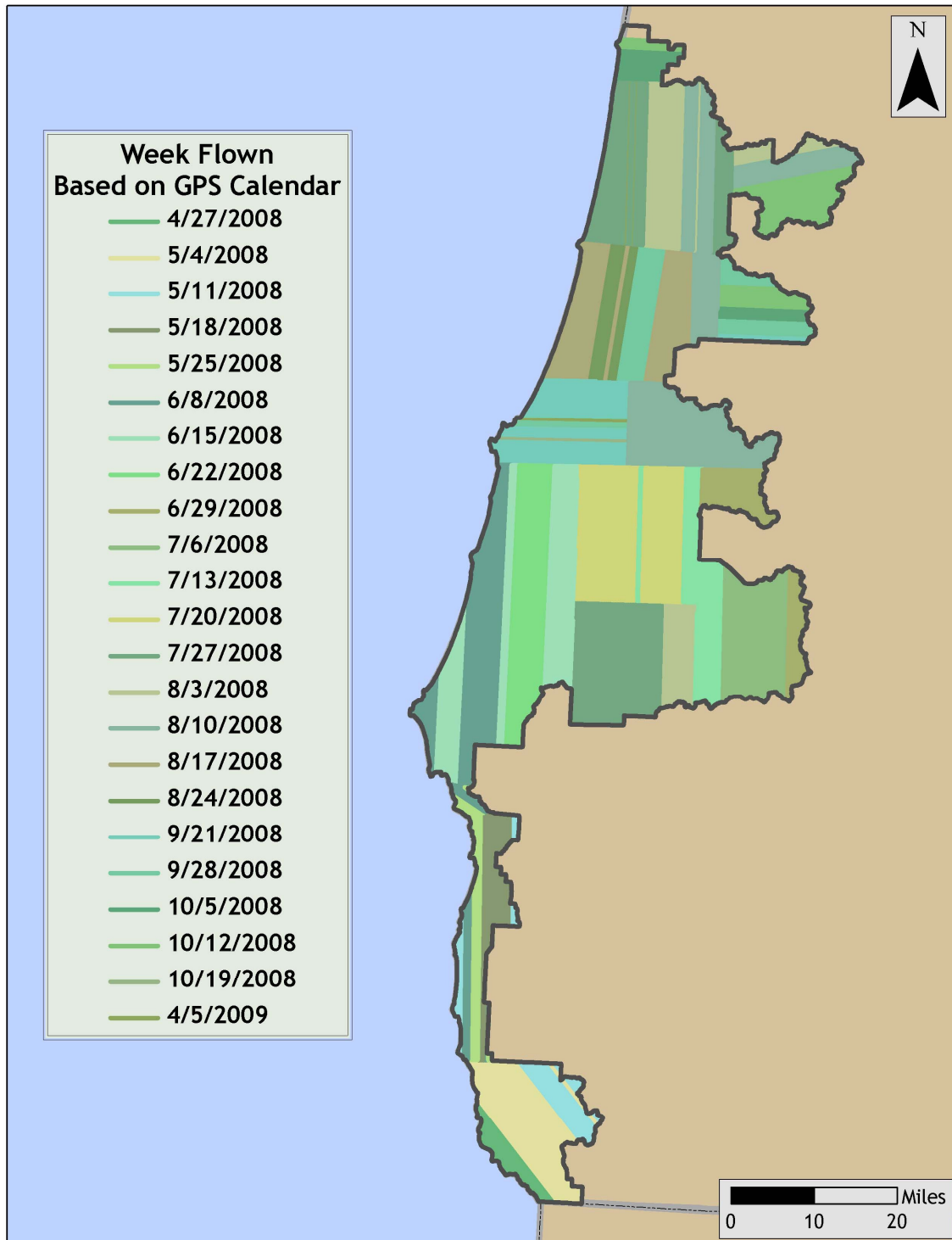


Table 1.2 (Continued from previous page). Base Station Surveyed Coordinates, (NAD83/NAVD88, OPUS corrected) used for kinematic post-processing of the aircraft GPS data for the South Coast study area.

Base Station ID	Datum NAD83(HARN)		GRS80
	Latitude (North)	Longitude (West)	Ellipsoid Height (m)
OLCCF2	42 57 55.66164	124 07 06.22758	102.674
OLCCF3	43 01 54.71258	124 06 43.96709	-7.289
OLCJN1	42 08 30.08496	124 12 49.11911	428.475
OLCJN2	42 08 27.95822	124 12 49.29884	427.870
OLCJN3	42 03 04.54697	124 17 30.17996	1.811
OLCJN4	42 03 50.25255	124 12 46.39603	31.933
OLCJN5	42 28 05.44507	124 20 46.24558	-21.890
OLCJN6	42 25 33.04097	124 25 35.72884	-19.346
OLCJN7	42 48 31.65550	124 29 21.62711	33.225
OLCJN8	43 09 26.13789	124 22 44.20041	-19.734
OLCJN9	42 47 10.43094	124 28 52.40738	-13.568
OLCJN10	43 00 44.63261	123 41 38.18942	307.728
OLCJN11	42 57 16.07660	123 46 38.70609	543.201
OLCPWH1	42 19 43.74040	124 25 33.76978	177.778
OLCPWH2	42 32 11.15305	124 23 59.59628	-13.175
OLCPWH3	42 27 48.10893	124 21 45.53382	-15.340
OLCPWH4	42 16 31.44293	124 24 15.39346	-21.678
OLCPWH5	42 48 26.82761	124 20 09.43708	68.264
OLCPWH6	43 07 56.53594	124 21 10.15905	-22.854
OLCPWH7	43 15 44.29178	123 49 12.34815	32.003
OLCPWH8	43 10 23.32427	124 12 00.96021	-19.743
OLCPWH9	42 59 01.23604	123 48 06.84695	733.518
OLCPWH10	43 15 44.25471	123 49 12.35897	285.251
OLCPWH11	43 09 54.31855	124 02 56.98822	62.611
OLCPWH12	43 15 44.29178	123 49 12.34815	285.248
OLCPWH13	43 00 21.54079	123 53 20.67738	50.495
OLCPWH14	42 59 29.68950	123 50 23.50621	328.574
OLCPWH15	42 56 37.78974	124 05 51.77012	43.503
OLCPWH16	42 54 02.56554	124 07 27.51313	117.941
OLCPWH17	43 21 47.87472	124 04 51.53211	-19.865
OLCBTK1	42 07 32.49487	124 18 37.00074	295.173
OLCBTK2	42 04 08.31008	124 18 52.63704	-16.064
OLCBTK3	42 08 39.24373	124 21 22.62505	-6.578
OLCBTK4	42 02 44.62353	124 16 04.64324	-21.946
AA5136	42 52 23.01388	124 03 42.88679	64.842
NGS_PID_OA07	43 5 54.88105	124 24 55.03463	-0.860
DH7020	43 5 11.08316	124 24 26.18403	7.977
6NCM2	43 42 14.56952	124 06 17.75696	-19.441

For data delivered to date, 20,024 RTK points were collected in the study area. Figures 1.6-1.11 show detailed views of RTK point locations.

Figure 1.6. RTK point locations in the study area; images are NAIP Orthoimages.

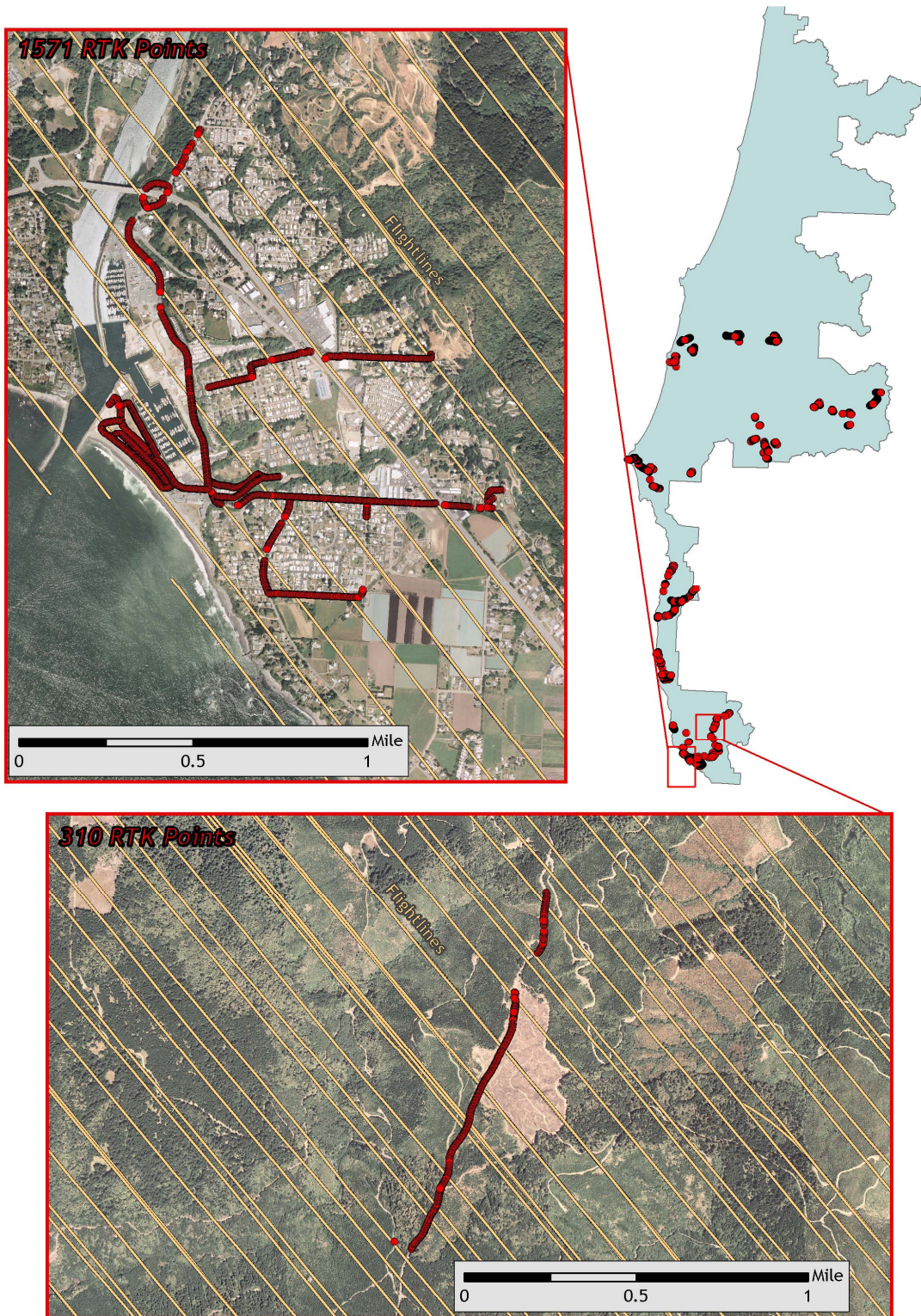


Figure 1.7. RTK point locations in the study area; images are NAIP Orthoimages.

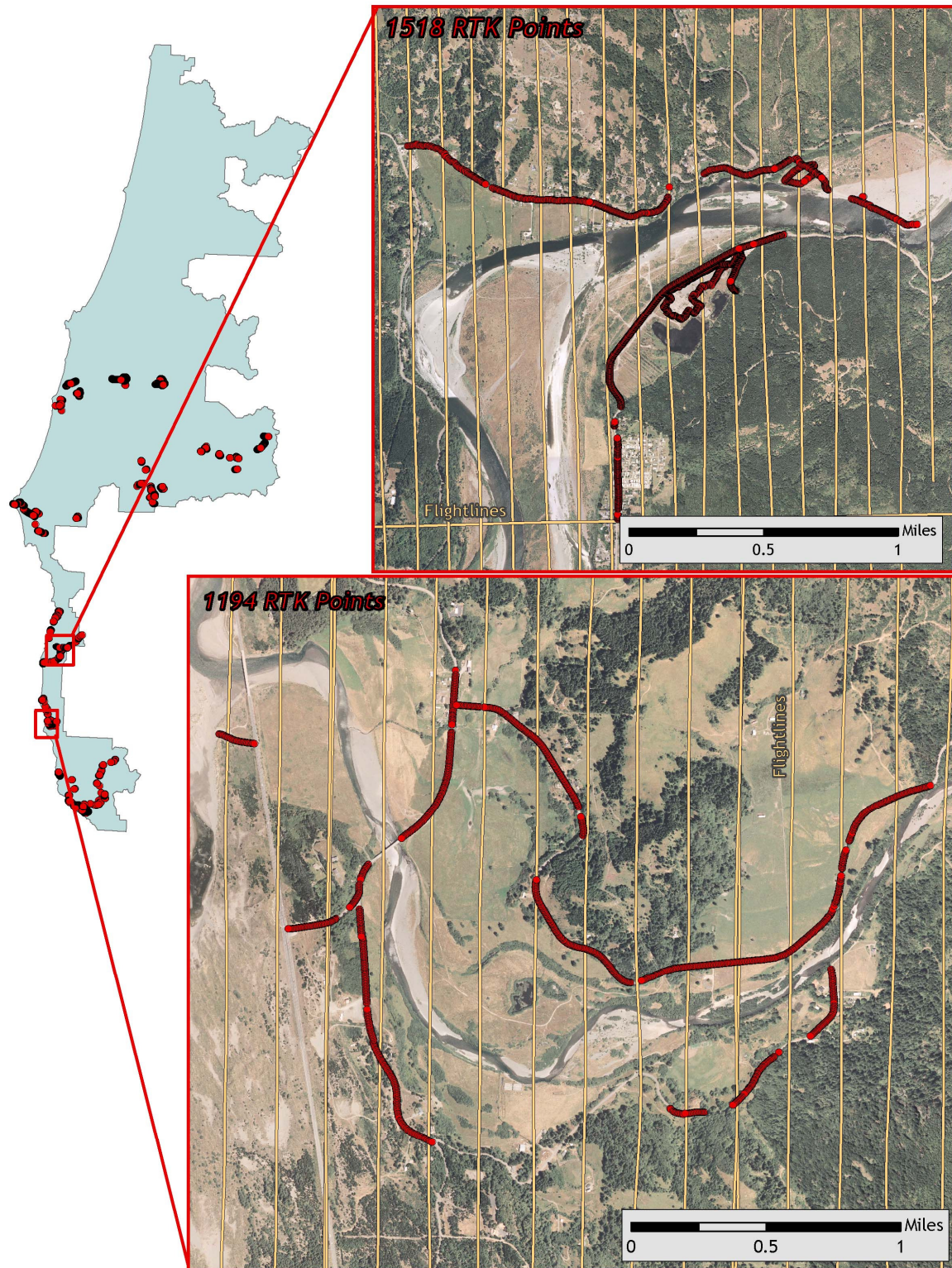


Figure 1.8. RTK point locations in the study area; images are NAIP Orthoimages.

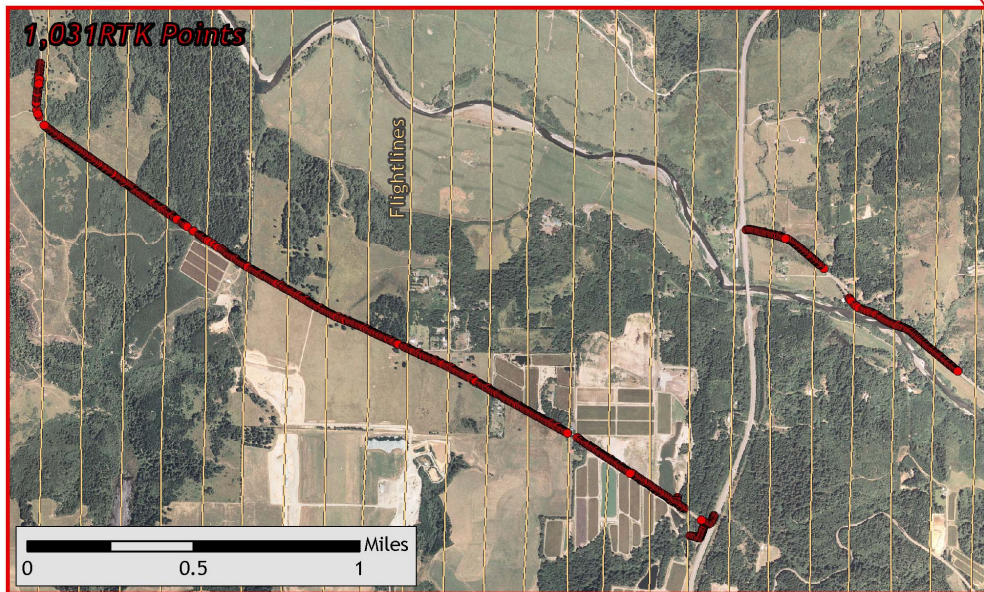
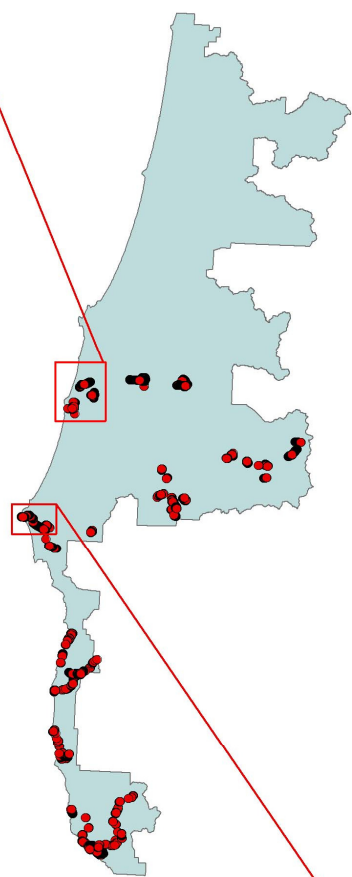


Figure 1.9. RTK point locations in the study area; images are NAIP Orthoimages.

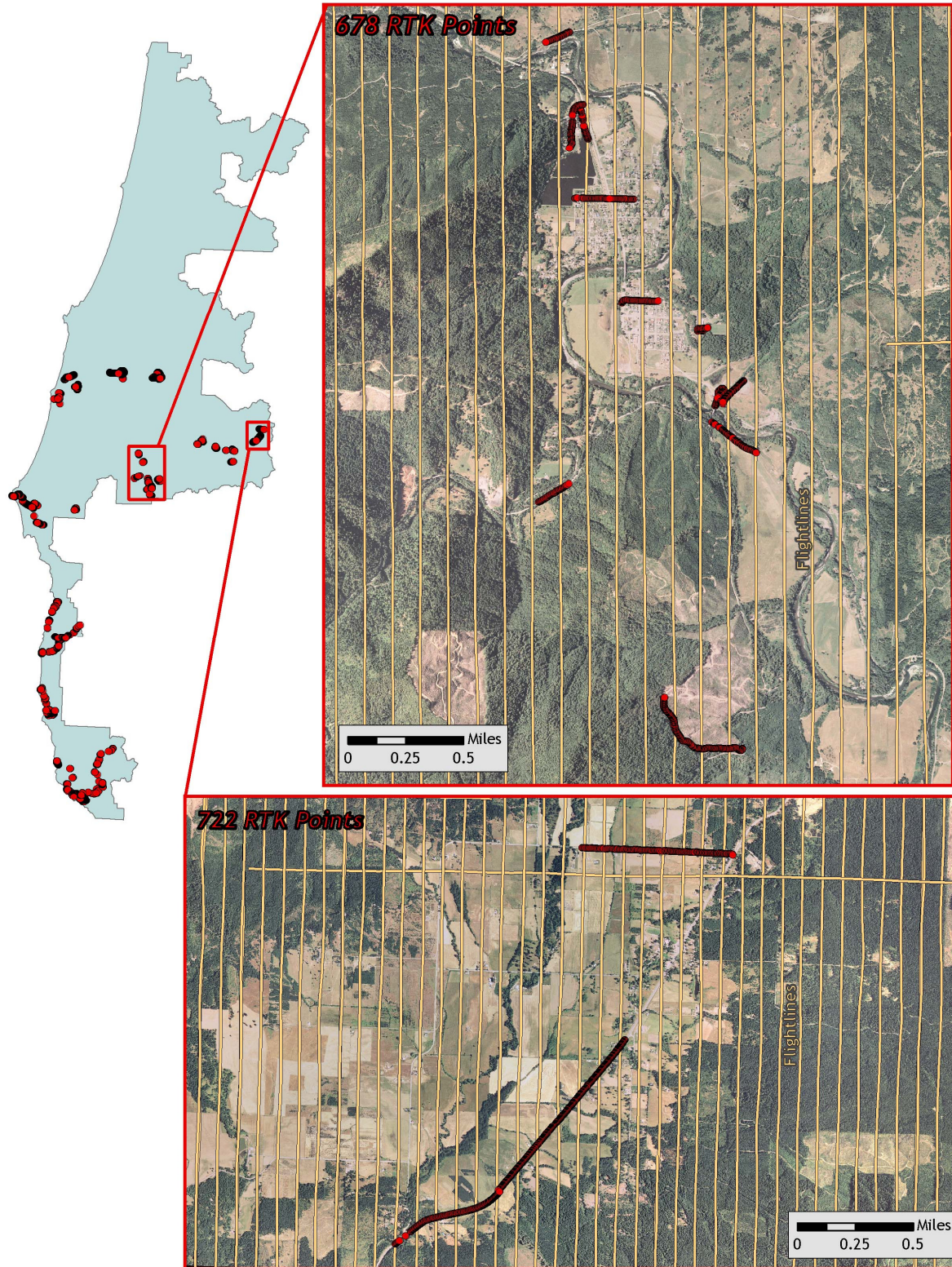


Figure 1.10. RTK point locations in the study area; images are NAIP Orthoimages.

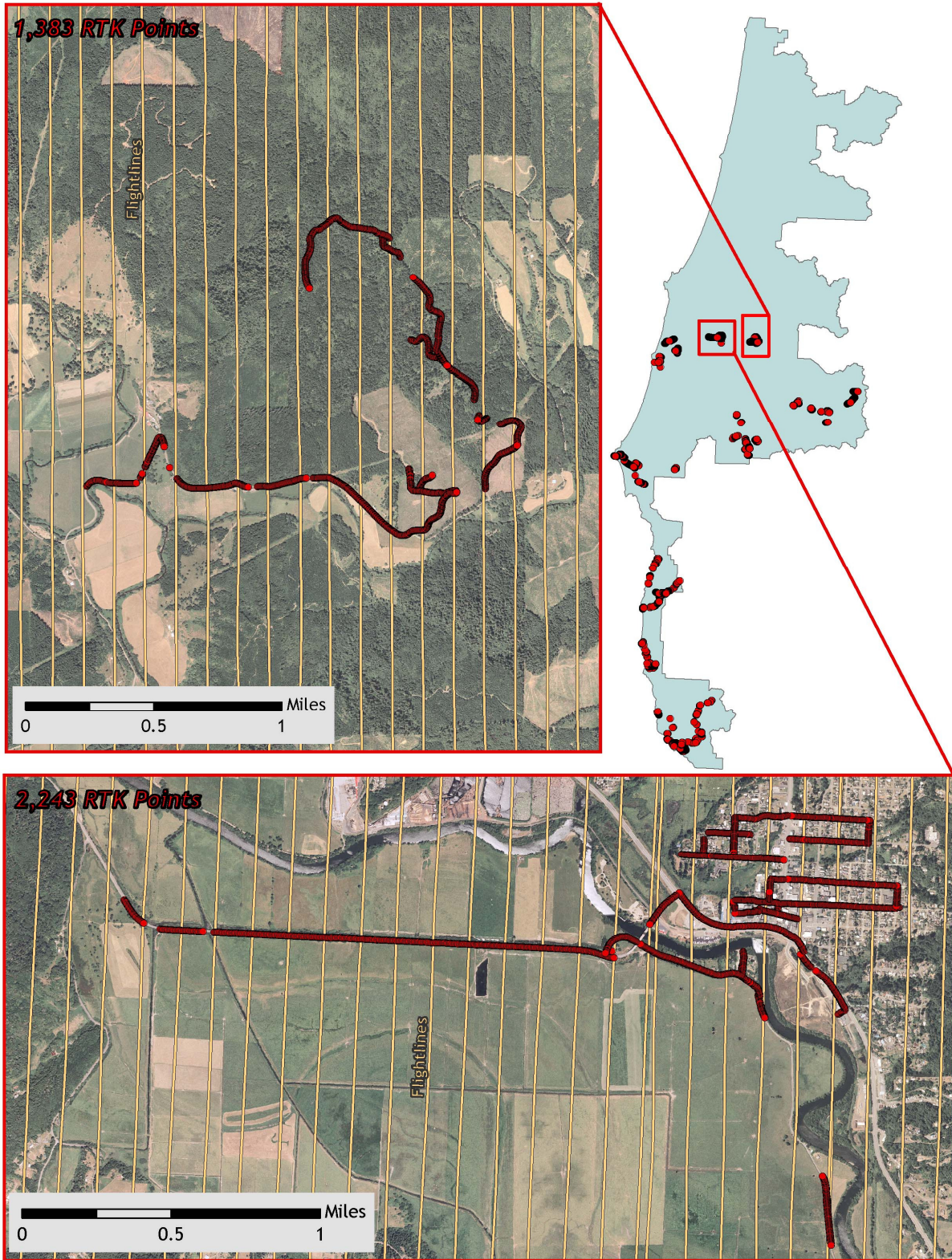
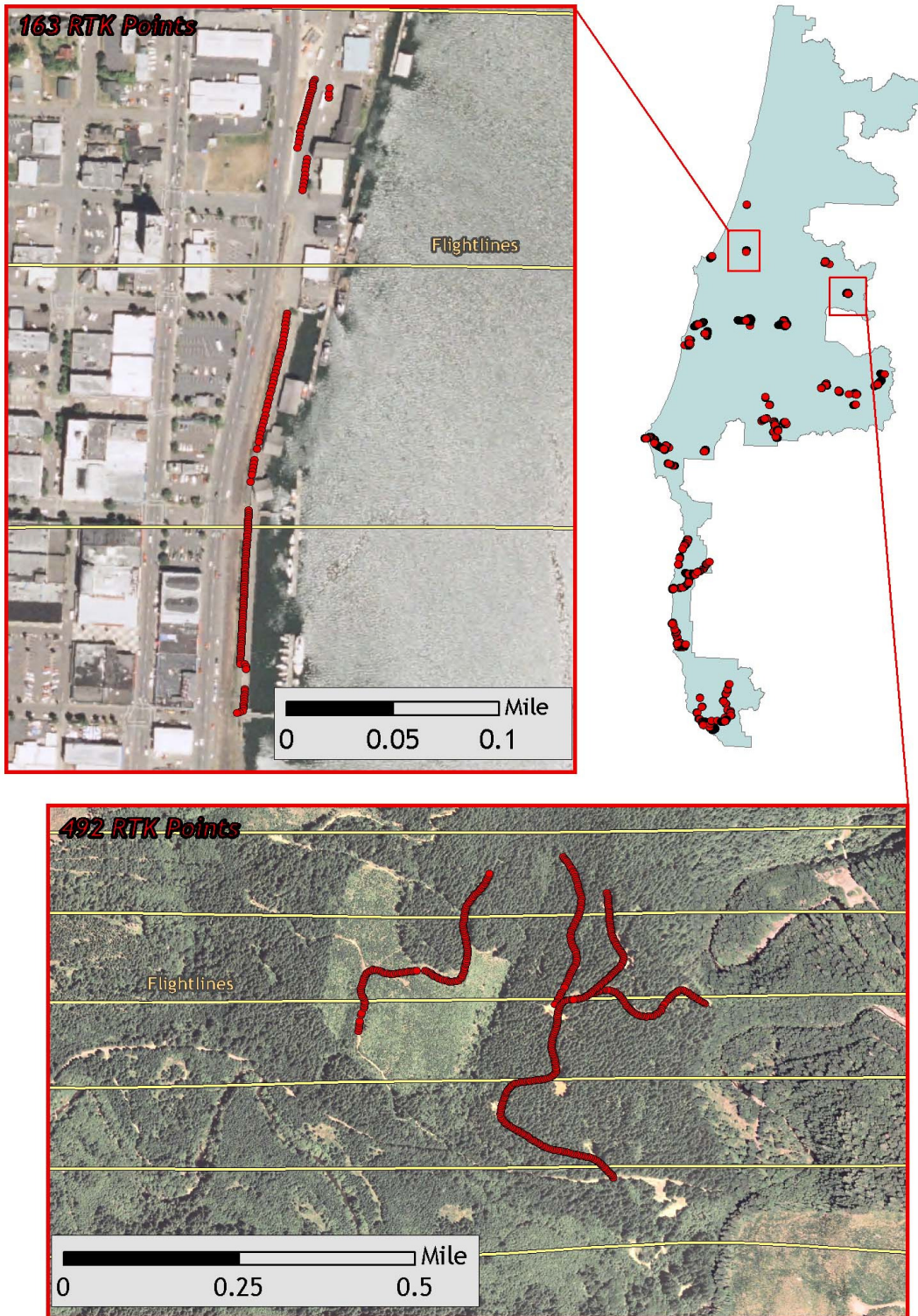


Figure 1.11. RTK point locations in the study area; images are NAIP Orthoimages.



2. Accuracy

2.1 Relative Accuracy

Relative accuracy statistics evaluate internal consistency (line to line reproducibility) for a LiDAR dataset, and are measured as the divergence between points from distinct, overlapping flightlines. The final report will include relative accuracy statistics for the entire South Coast study area. To date, reported project averages are well within contracted specifications.

2.2 Absolute Accuracy

Absolute accuracy compares known Real Time Kinematic (RTK) ground survey points to the closest laser point. For the South Coast study area, 20,024 RTK points were collected for data delivered to date. Accuracy statistics are reported in Table 2.1 and shown in Figures 2.3-2.3.

Table 2.1. Absolute Accuracy - Deviation between laser points and RTK survey points.

Sample Size (n): 20,024	
Root Mean Square Error (RMSE): 0.14 feet (0.04 meters)	
Standard Deviations	Deviations
1 sigma (σ): 0.14 feet (0.04 meters)	Minimum Δz : -0.66 feet (-0.20 meters)
2 sigma (σ): 0.10 feet (0.32 meters)	Maximum Δz : 0.67 feet (0.20 meters)
	Average Δz : 0.12 feet (0.04 meters)

Figure 2.1. Portion of the study area for which absolute accuracy statistics are reported.

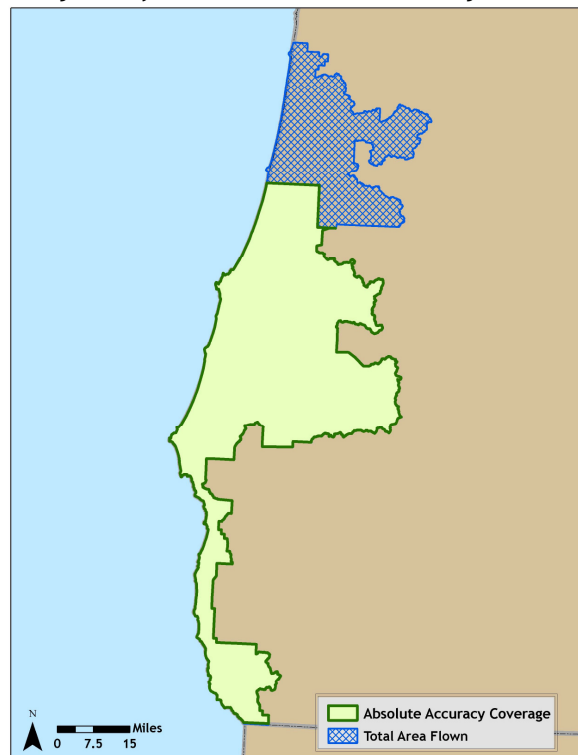


Figure 2.2. South Coast Study area histogram statistics

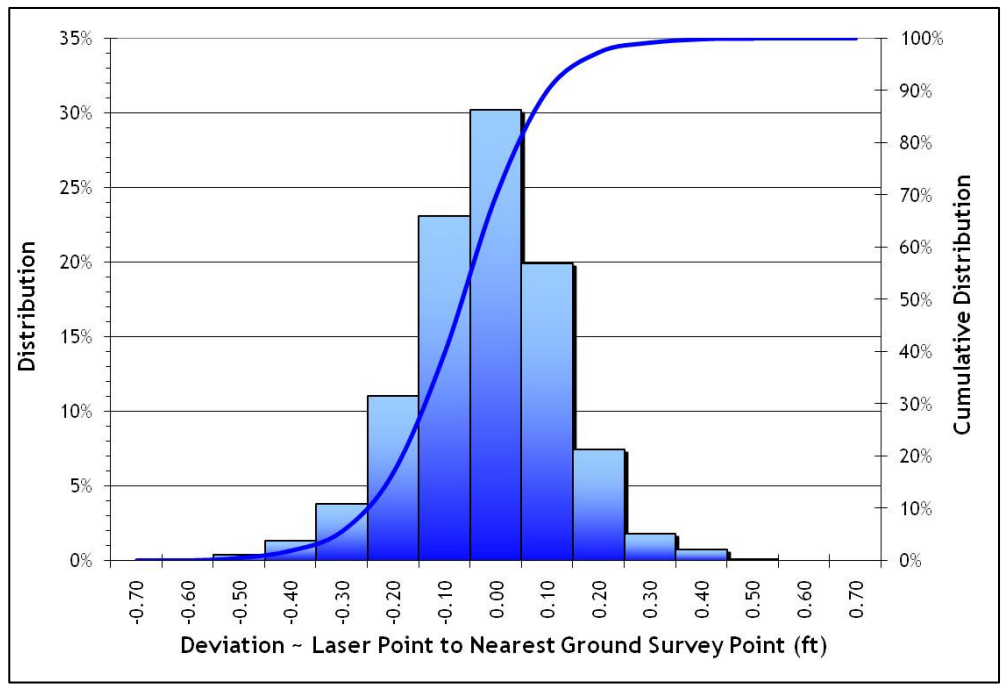
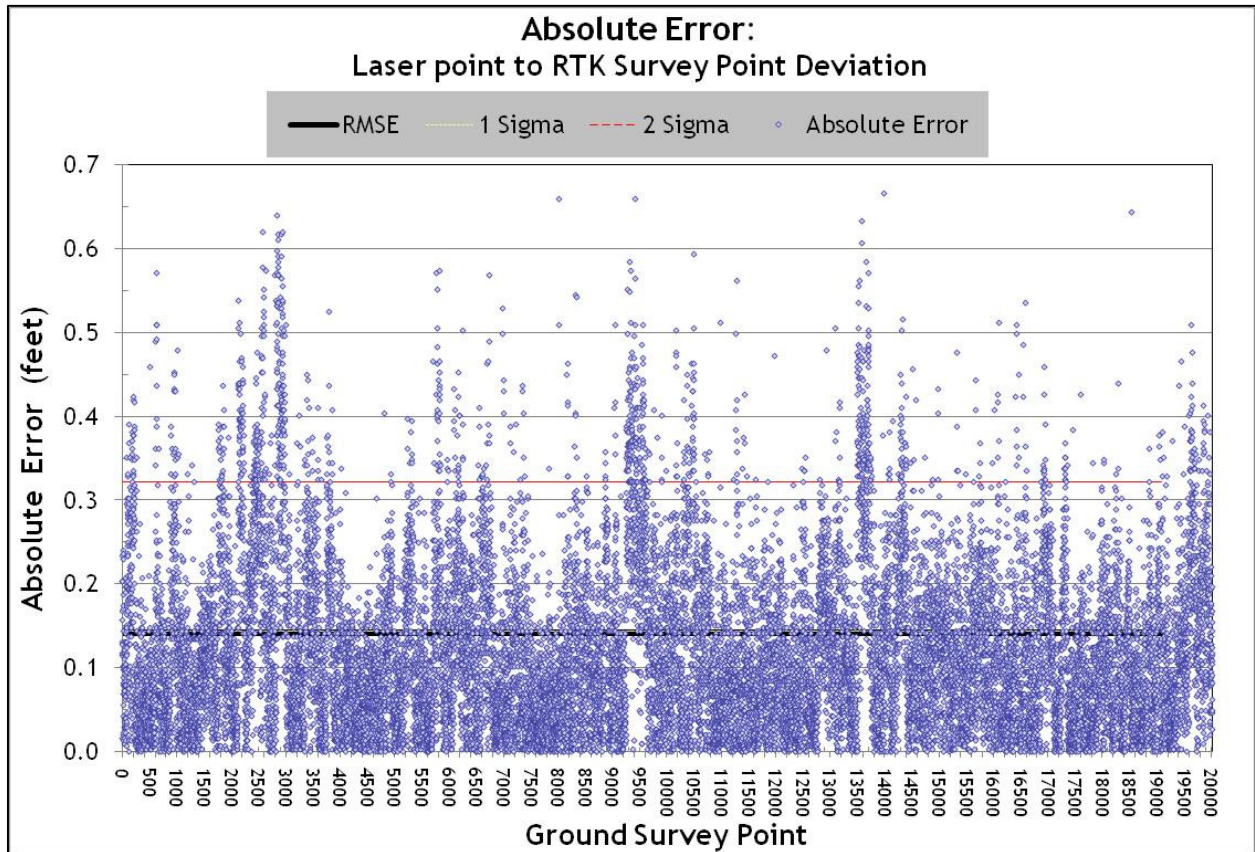


Figure 2.3. South Coast study area point absolute deviation statistics.



3. Data Density/Resolution

3.1 Density Statistics

Some types of surfaces (i.e., dense vegetation or water) may return fewer pulses than the laser originally emitted. Therefore, the delivered density can be less than the native density and vary according to distributions of terrain, land cover and water bodies. Density histograms and maps (Figures 3.1 - 3.4) have been calculated based on first return laser point density and ground-classified laser point density.

Table 3.1. Average density statistics for South Coast data delivered to date.

Average Pulse Density (per square ft)	Average Pulse Density (per square m)	Average Ground Density (per square ft)	Average Ground Density (per square m)
0.77	8.28	0.06	0.69

Figure 3.1. Histogram of first return laser point density for data delivered to date.

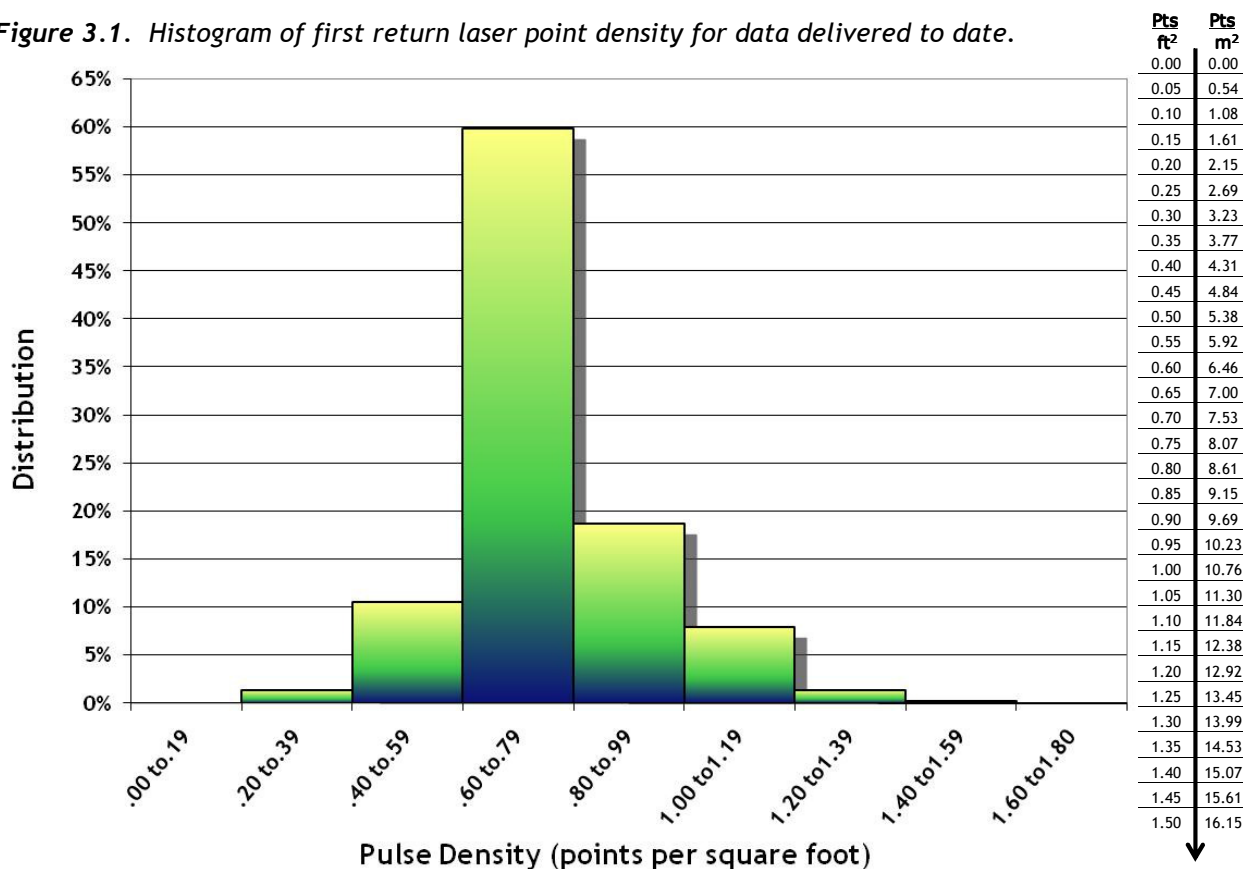
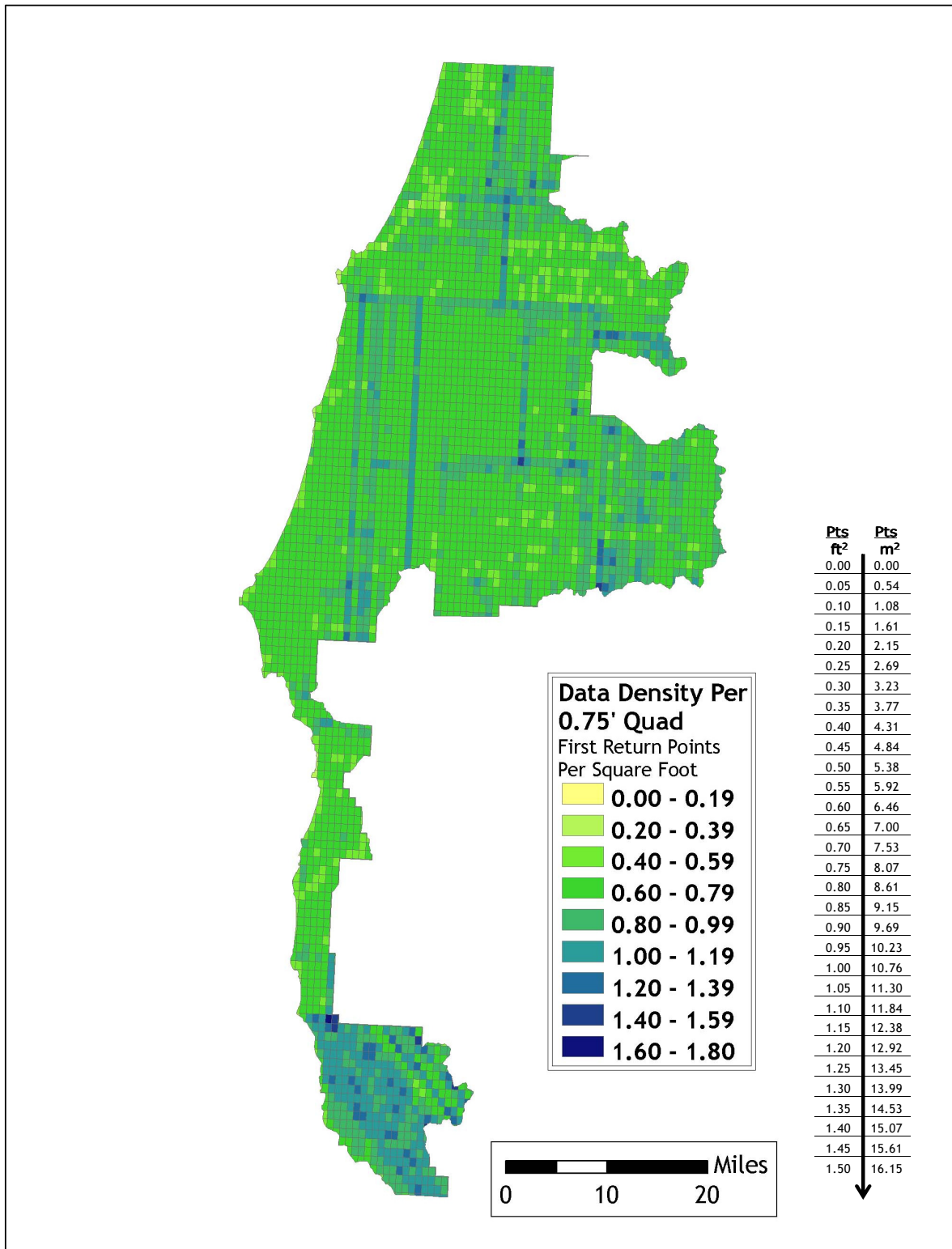
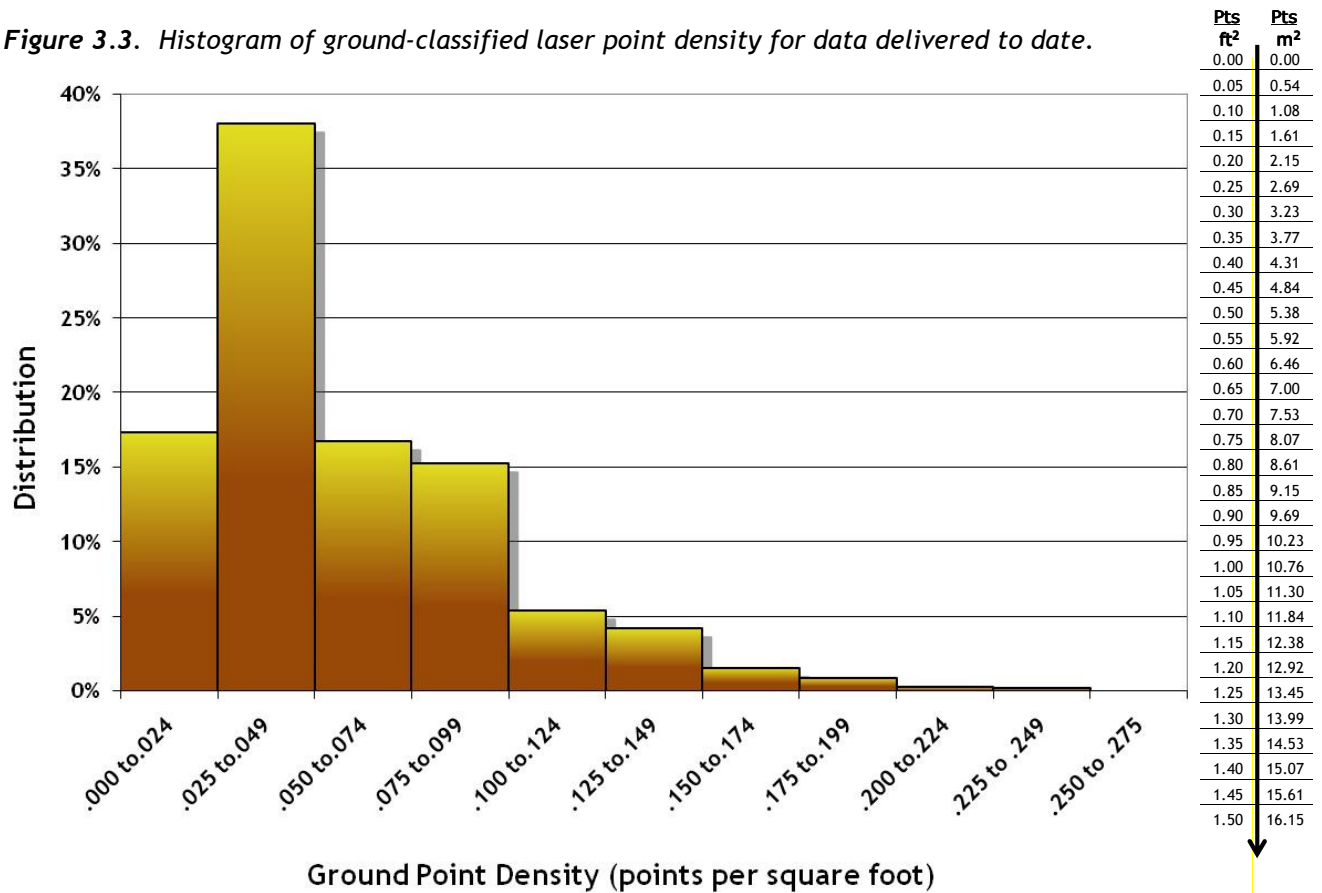


Figure 3.2. Image shows first return laser point per 0.75' USGS Quad for data delivered to date.



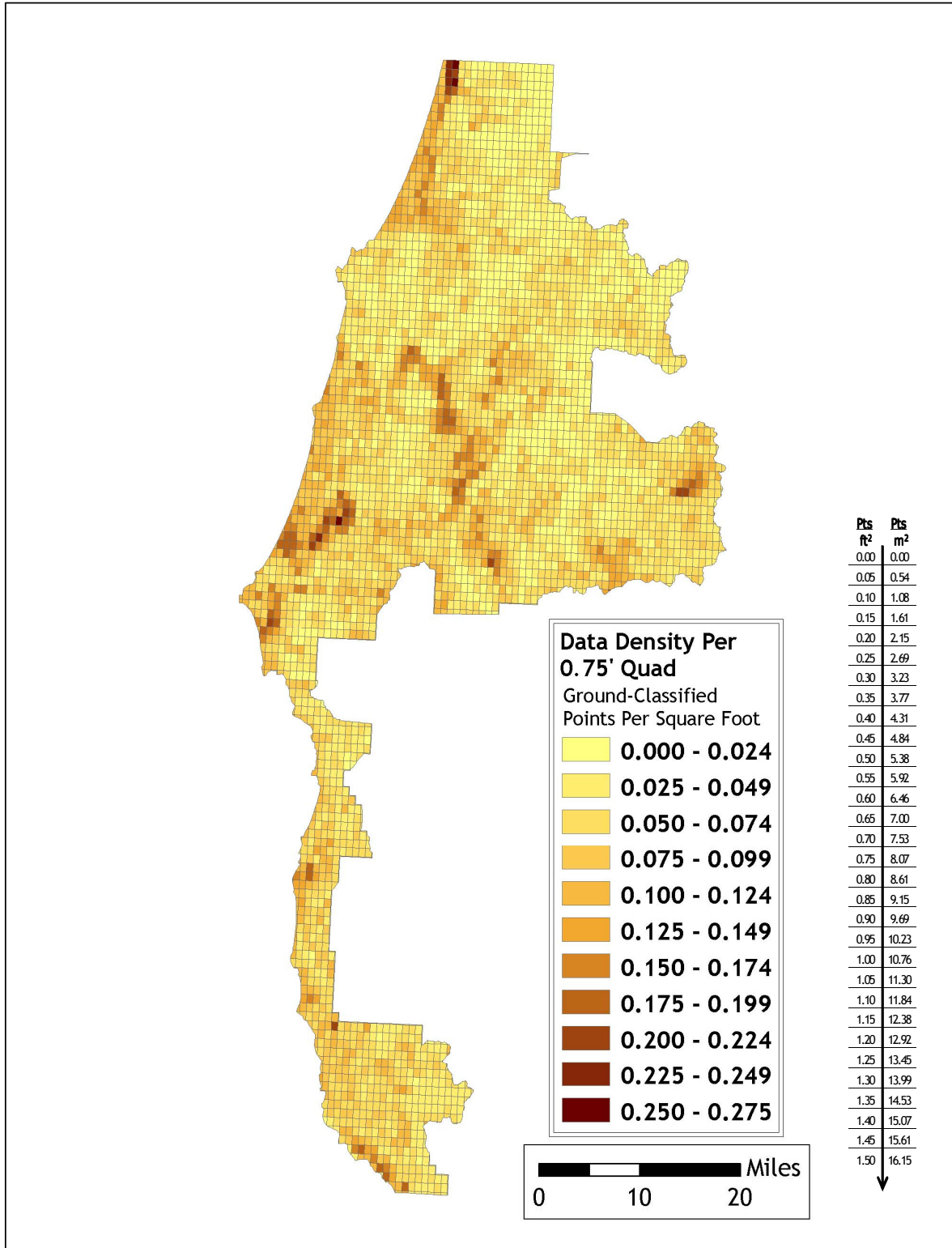
Ground classifications were derived from ground surface modeling. Supervised classifications were performed by reseeded of the ground model where it was determined that the ground model failed, usually under dense vegetation and/or at breaks in terrain, steep slopes and at bin boundaries.

Figure 3.3. Histogram of ground-classified laser point density for data delivered to date.



Pts ft ²	Pts m ²
0.00	0.00
0.05	0.54
0.10	1.08
0.15	1.61
0.20	2.15
0.25	2.69
0.30	3.23
0.35	3.77
0.40	4.31
0.45	4.84
0.50	5.38
0.55	5.92
0.60	6.46
0.65	7.00
0.70	7.53
0.75	8.07
0.80	8.61
0.85	9.15
0.90	9.69
0.95	10.23
1.00	10.76
1.05	11.30
1.10	11.84
1.15	12.38
1.20	12.92
1.25	13.45
1.30	13.99
1.35	14.53
1.40	15.07
1.45	15.61
1.50	16.15

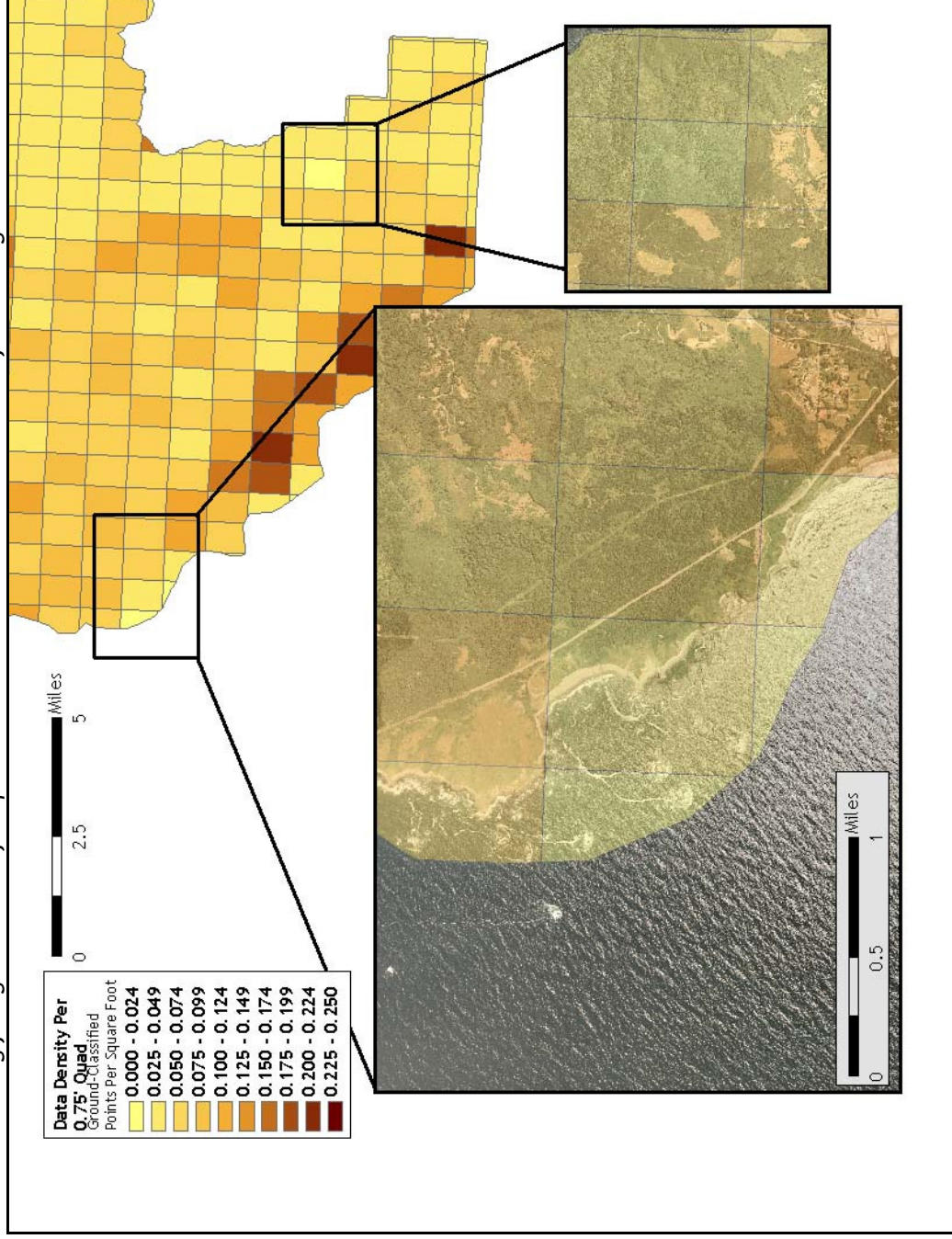
Figure 3.4. Ground-classified laser point density per 0.75' USGS Quad for data delivered to date.



3.2 Data Density/Resolution per Delivery

3.2.1 Delivery 1

Figure 3.5. Quadrants containing few ground classified points include coastal areas and areas of dense vegetation.



3.2.2 Delivery 2

Figure 3.6. This quadrant illustrates a high number of ground classified points due to flightline overlap and areas of little or no ground cover.

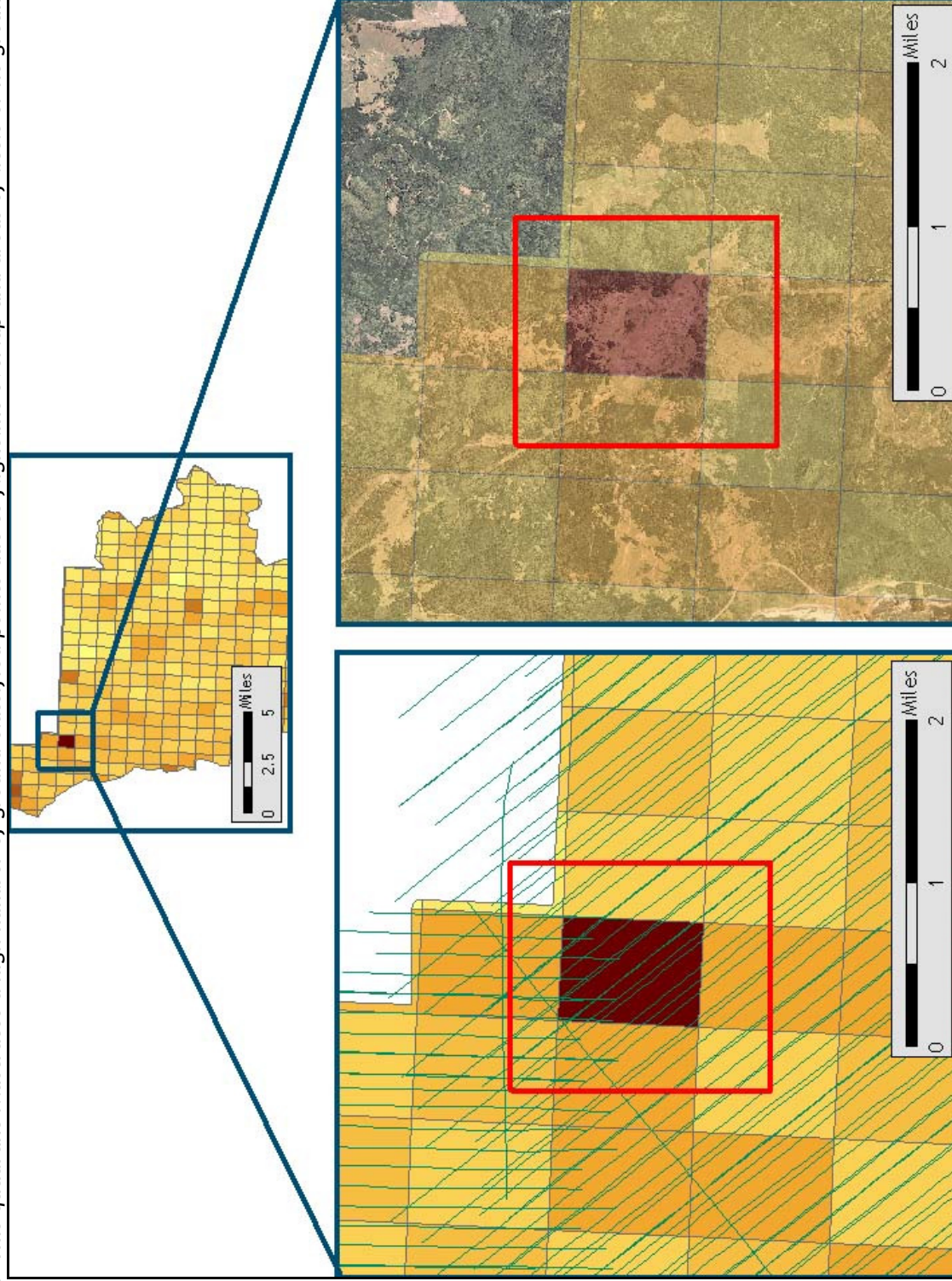
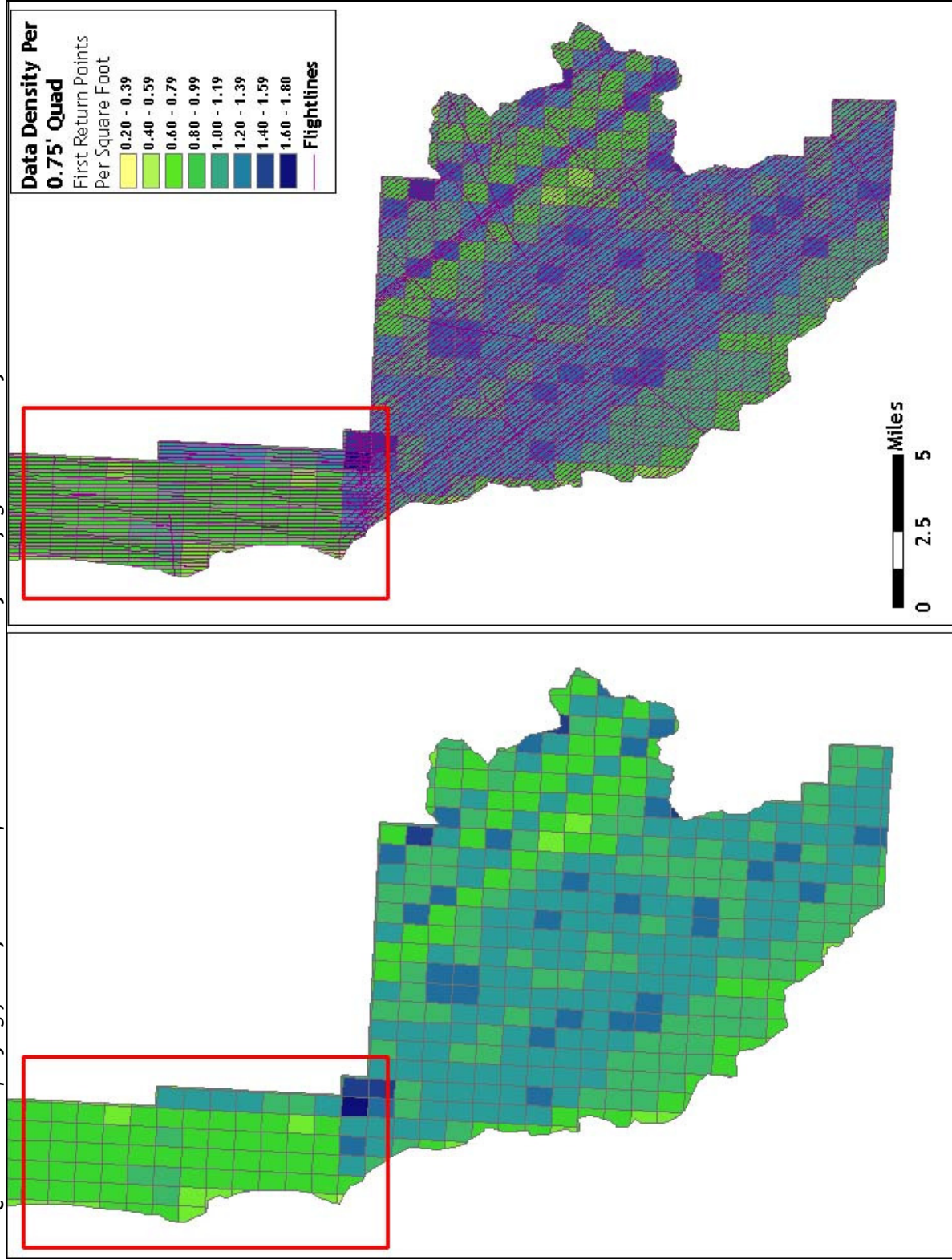
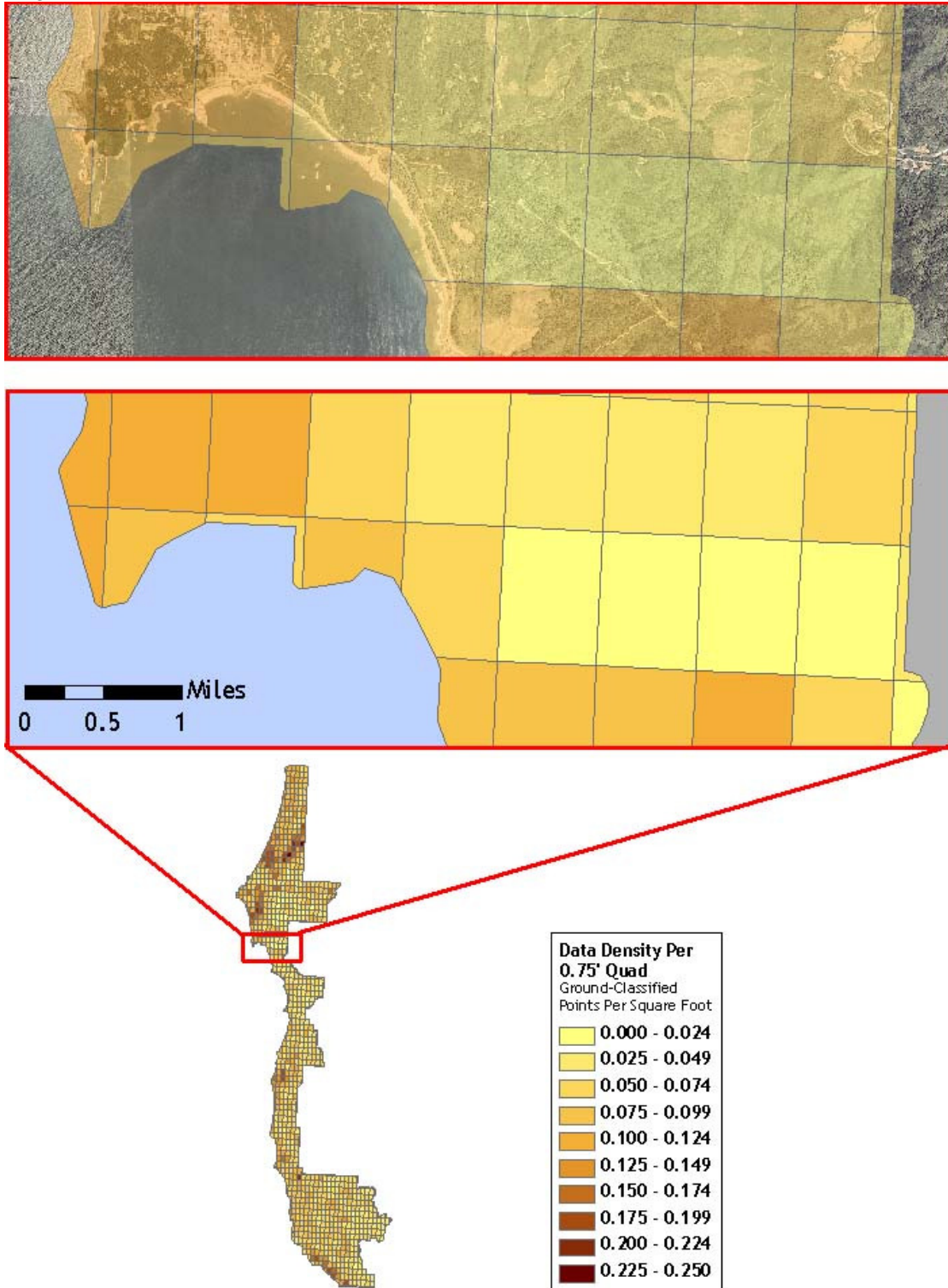


Figure 3.7. Quadrants displaying fewer first return points correlate directly with flightline density.



3.2.3 Delivery 3

Figure 3.8. Quadrants containing few ground classified points include coastal areas and areas of dense vegetation.



3.2.4 Delivery 4

Figure 3.9. Quadrants with exposed ground or little vegetation result in higher ground-classified point density.

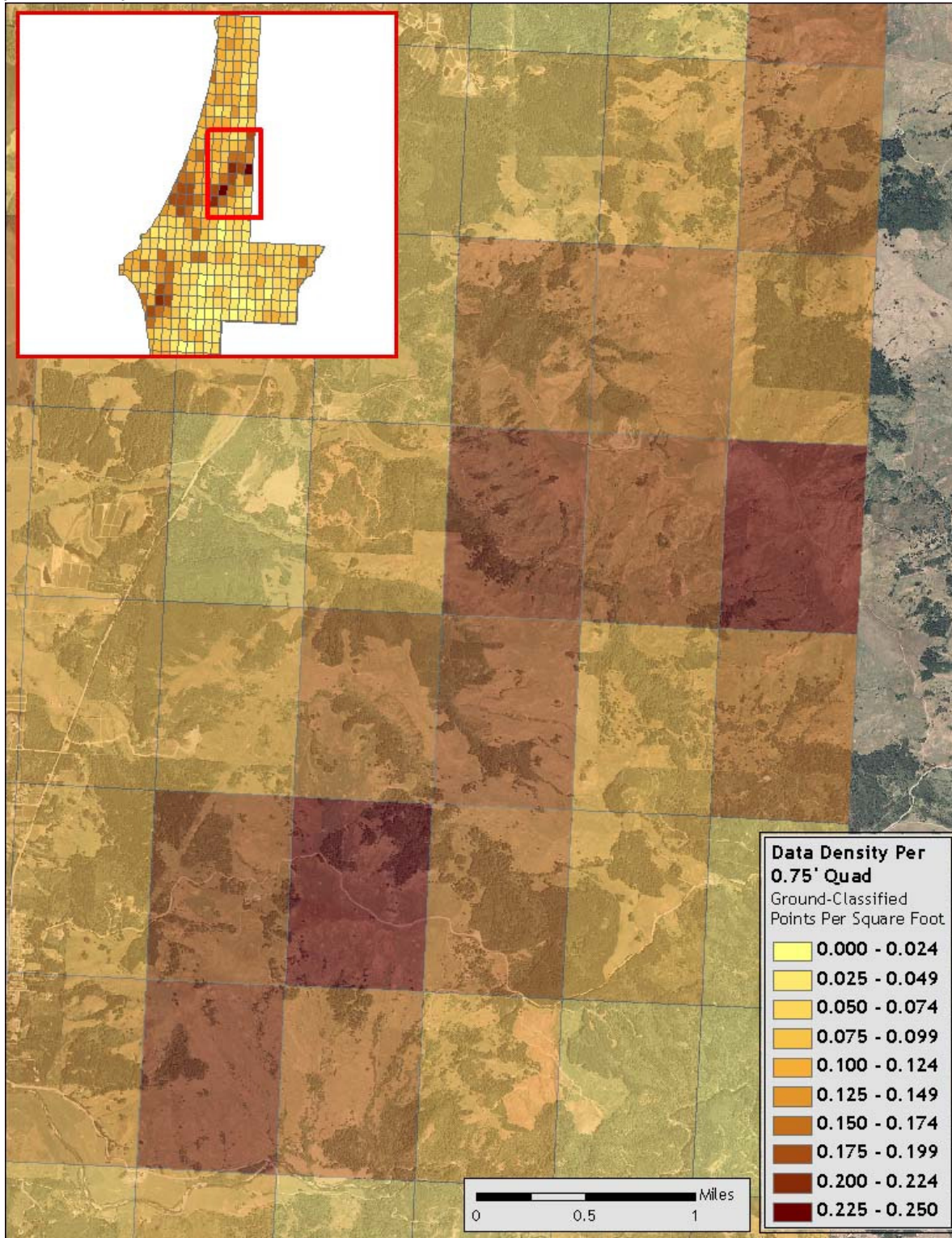
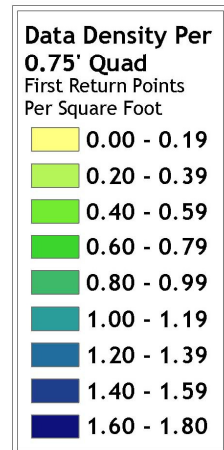
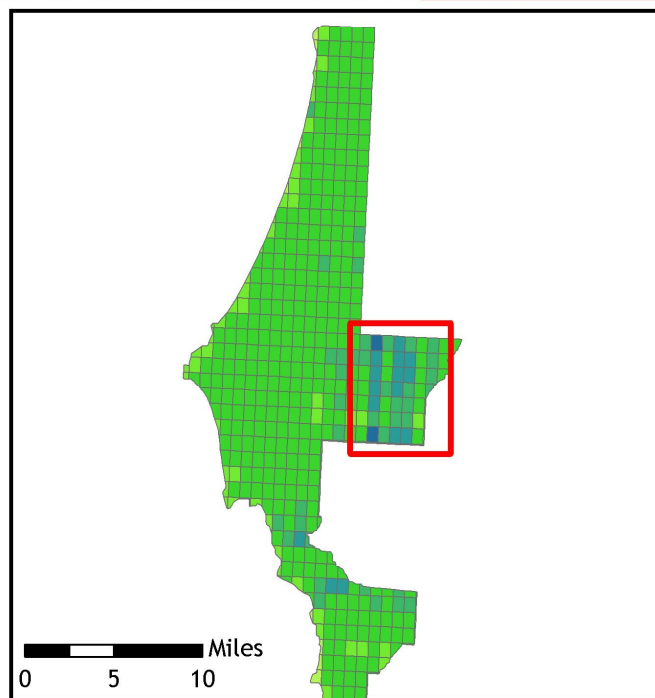
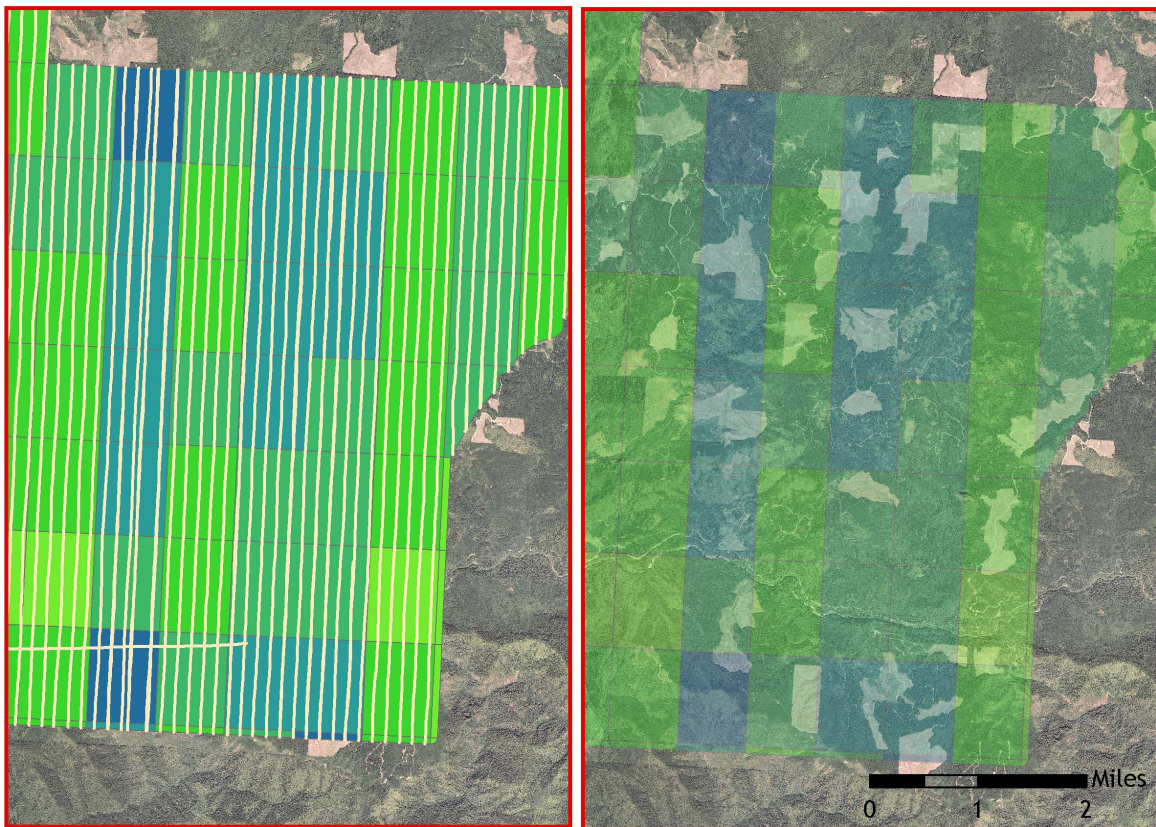


Figure 3.10. Quadrants with higher flightline density result in greater numbers of first return points.



4. Selected Imagery

Example areas are presented to show sample imagery (see Figures 4.1-4.13).

Figure 4.1. View to Northwest at oceanside near Harris Beach State Park, Oregon (quad 42124-A3). Top image derived from highest hit LiDAR, lower image derived from bare earth LiDAR.

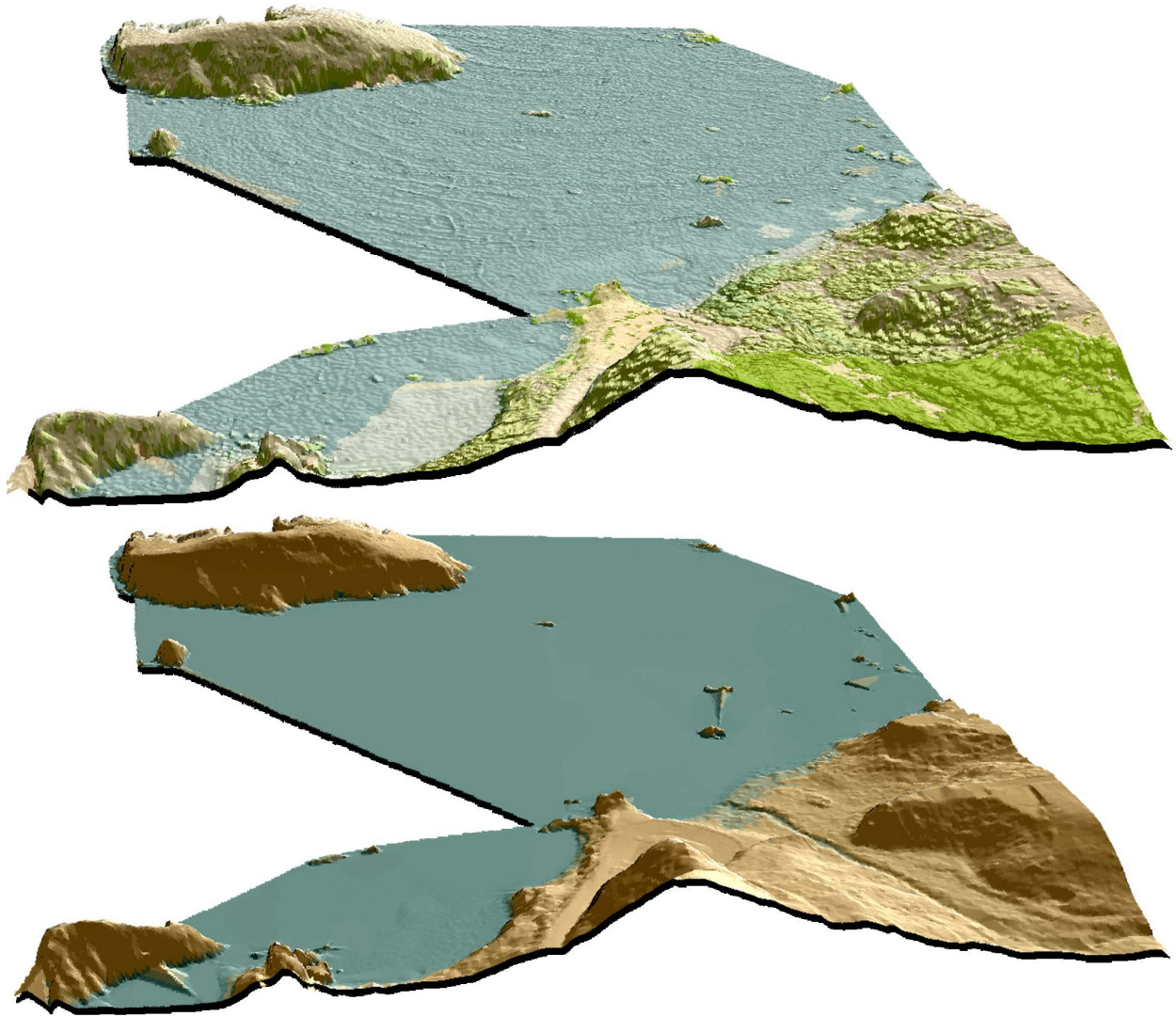


Figure 4.2. View to Southeast and upstream along Chetco River at its confluence with Jack Creek (quad 42124-A2). Top image is derived from highest hit LiDAR, lower image derived from bare earth LiDAR.

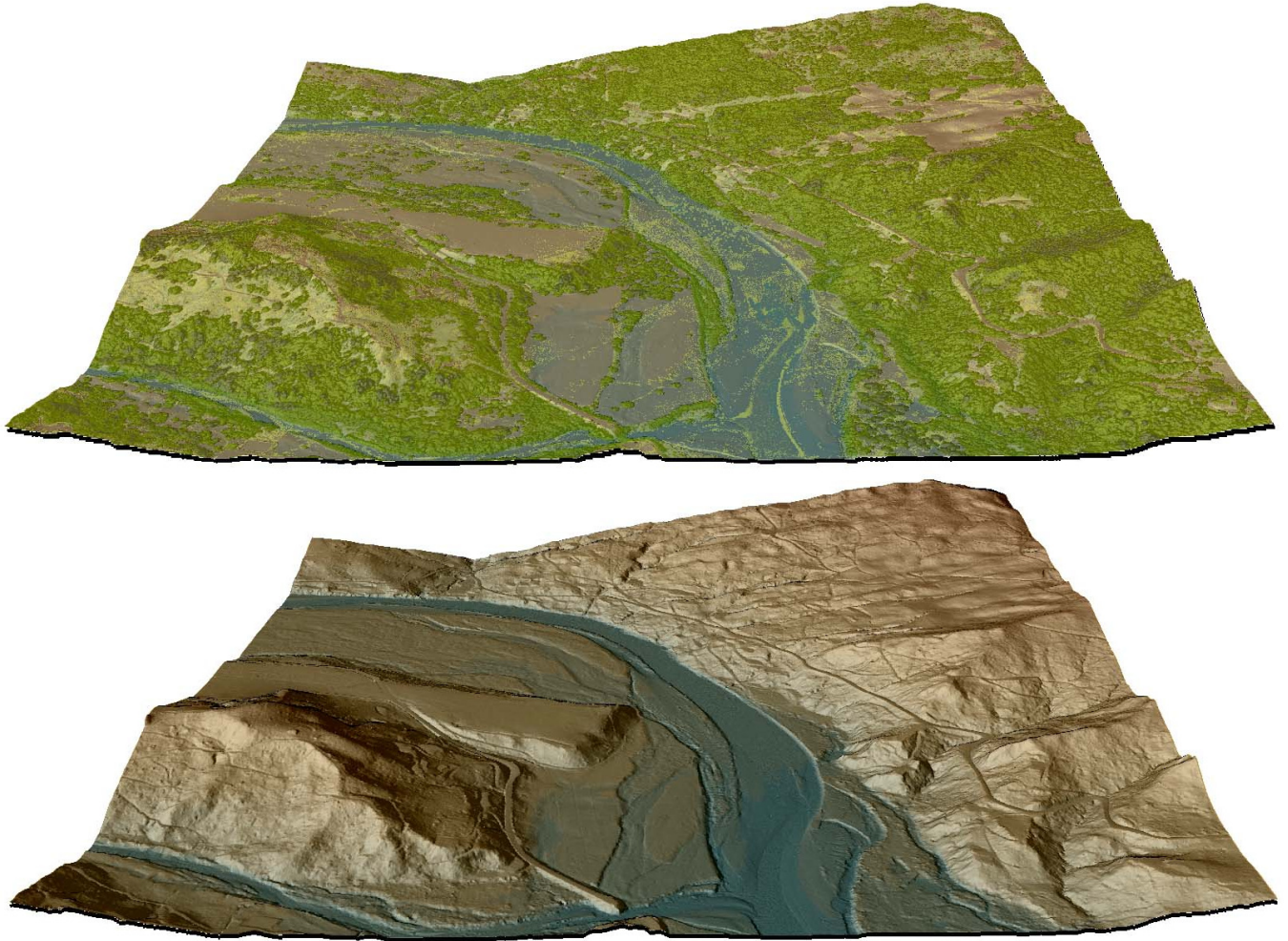


Figure 4.3. View upstream and to Northeast of Chetco River at confluence with North Fork Chetco River (quad 42124-a2). Top image derived from highest hit LiDAR, lower image derived from bare earth LiDAR.

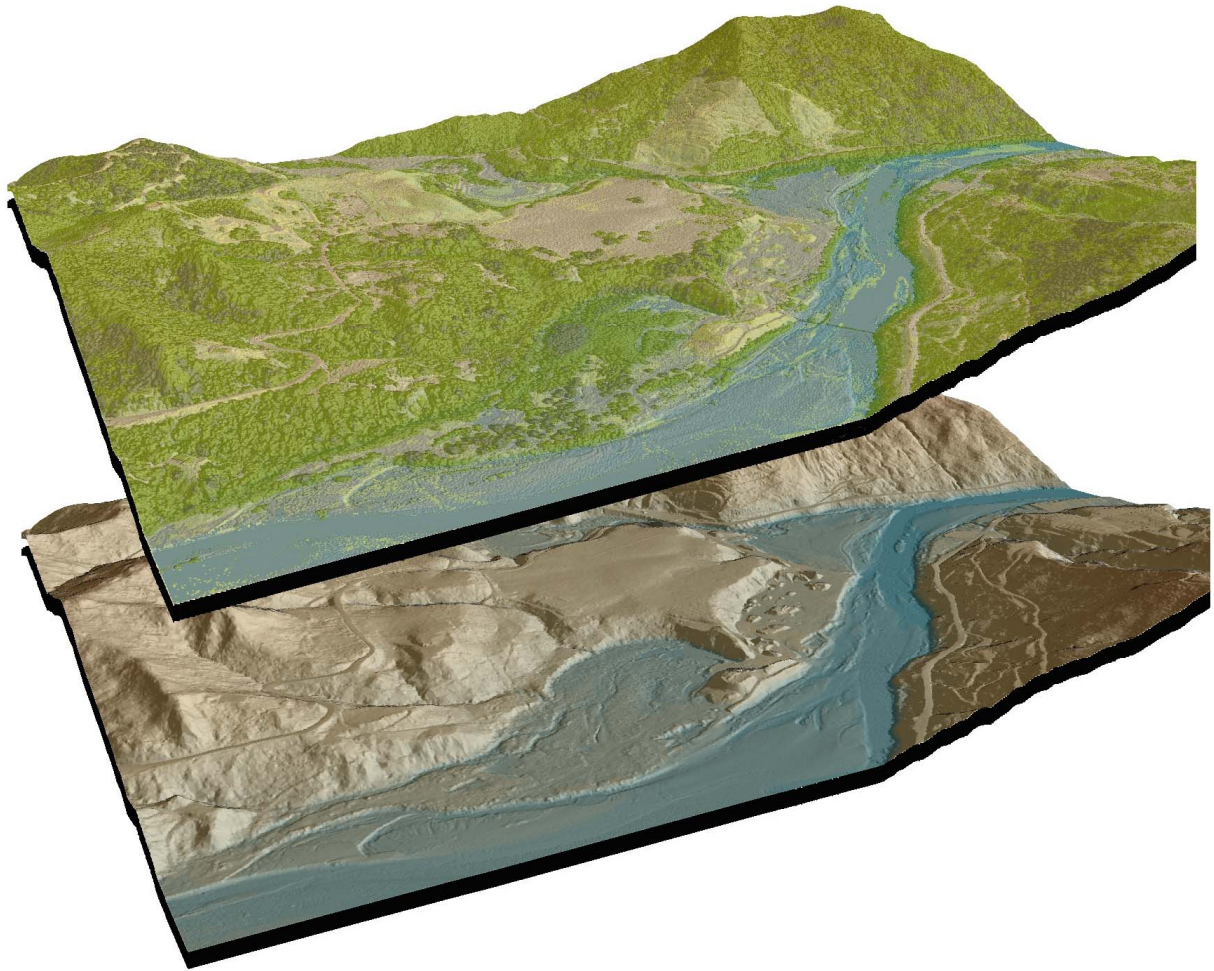


Figure 4.4. Oblique view of coastline at confluence of Whalehead Creek and ocean (quad 42124-b3). Upper image derived from highest hit LiDAR, lower image derived from bare earth LiDAR.

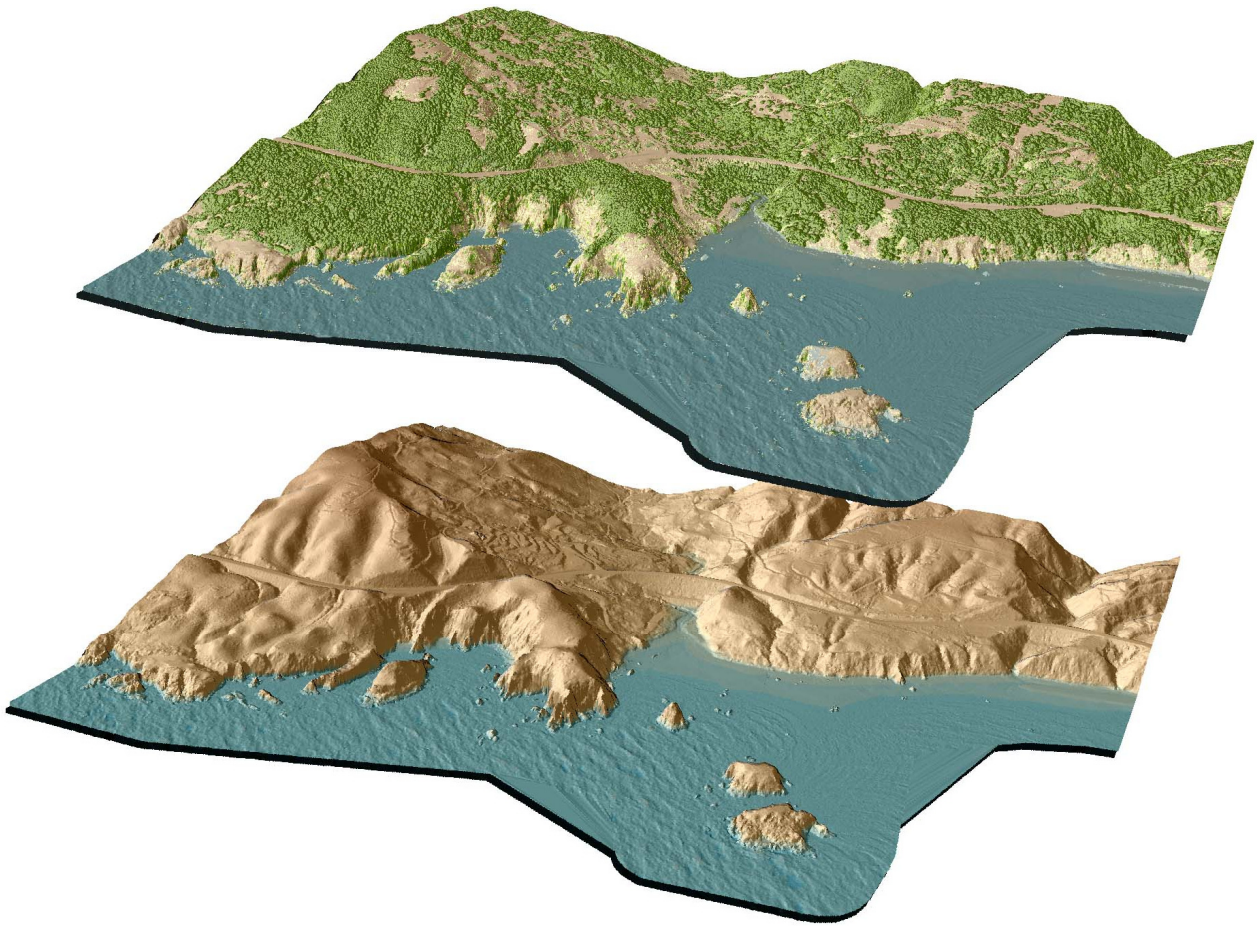


Figure 4.5. Oblique view to North over Chetco River and North Fork Chetco River (quad 42124-a2). Top image derived from LiDAR highest hits, bottom from bare earth LiDAR.

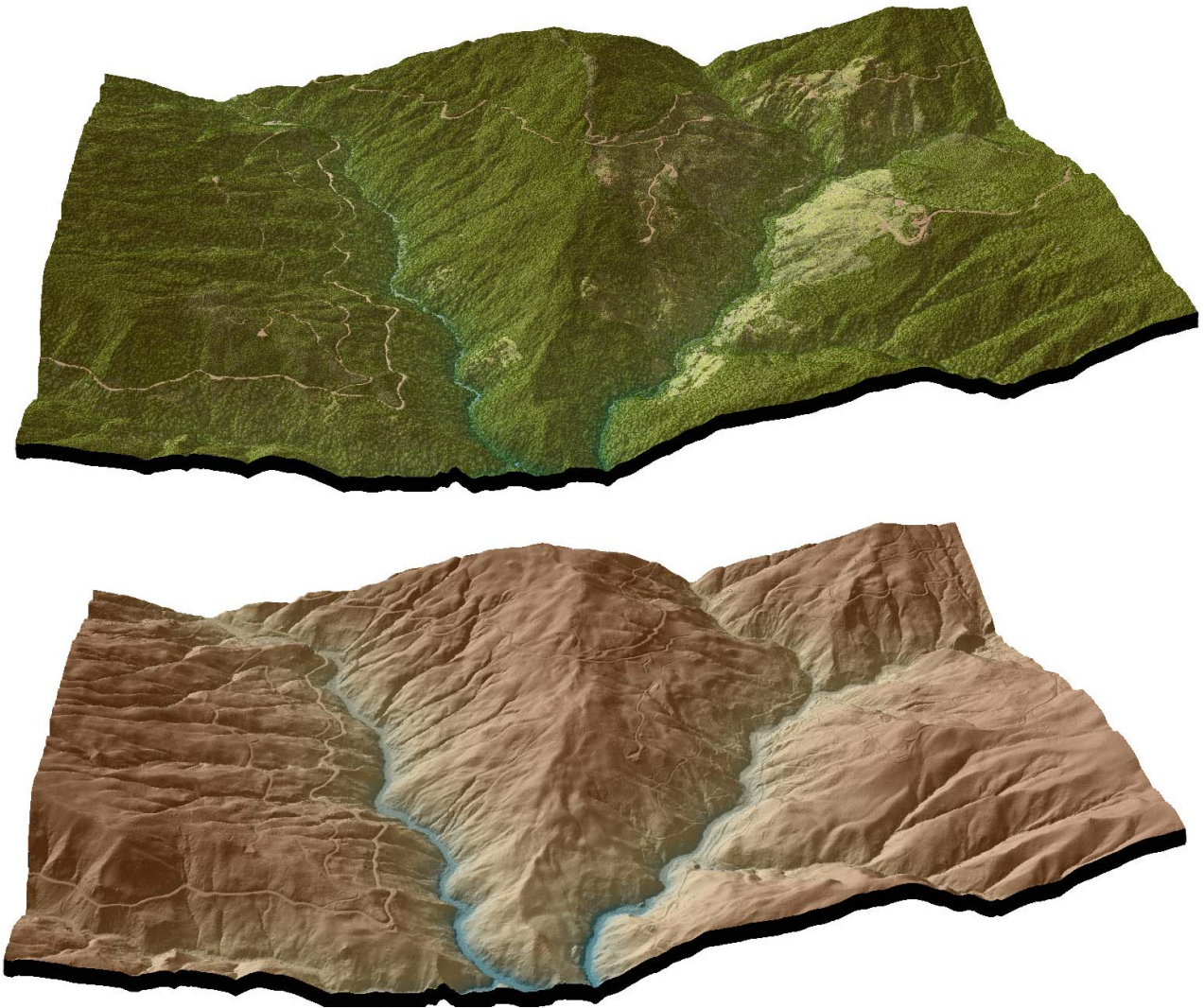


Figure 4.6. Cape Arago State Park, South Cove (Quad 43124C4). Top image derived from LiDAR highest hits, bottom from bare earth LiDAR.

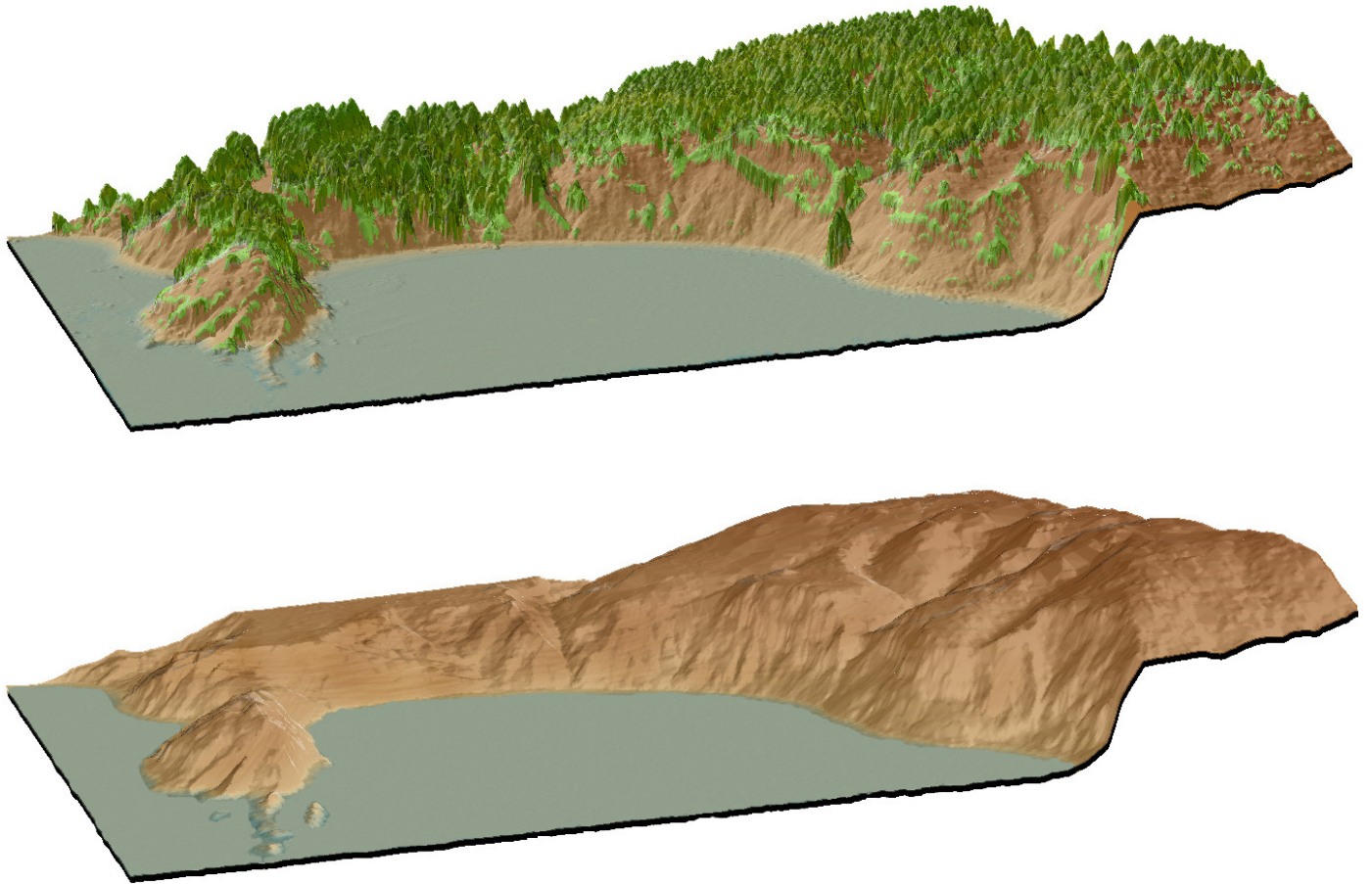


Figure 4.7. Chetco River upstream of confluence with Elk Creek (quad 42124-b2). Upper image derived from highest hit LiDAR, center image derived from bare earth LiDAR, lower image derived from NAIP orthophoto.



Figure 4.8. Whalehead and Coon Creek at terminus in ocean near Highway 101 (quad42124-b3). Top image derived from highest hit LiDAR, center image from bare earth LiDAR, lower image derived from NAIP orthophotos.



Figure 4.9. View of the Sixes River and Bea Creek confluence in delivery tile 42124g3. Top image derived from bare earth LiDAR, center image from highest hit LiDAR, and lower image derived from NAIP orthophotos.

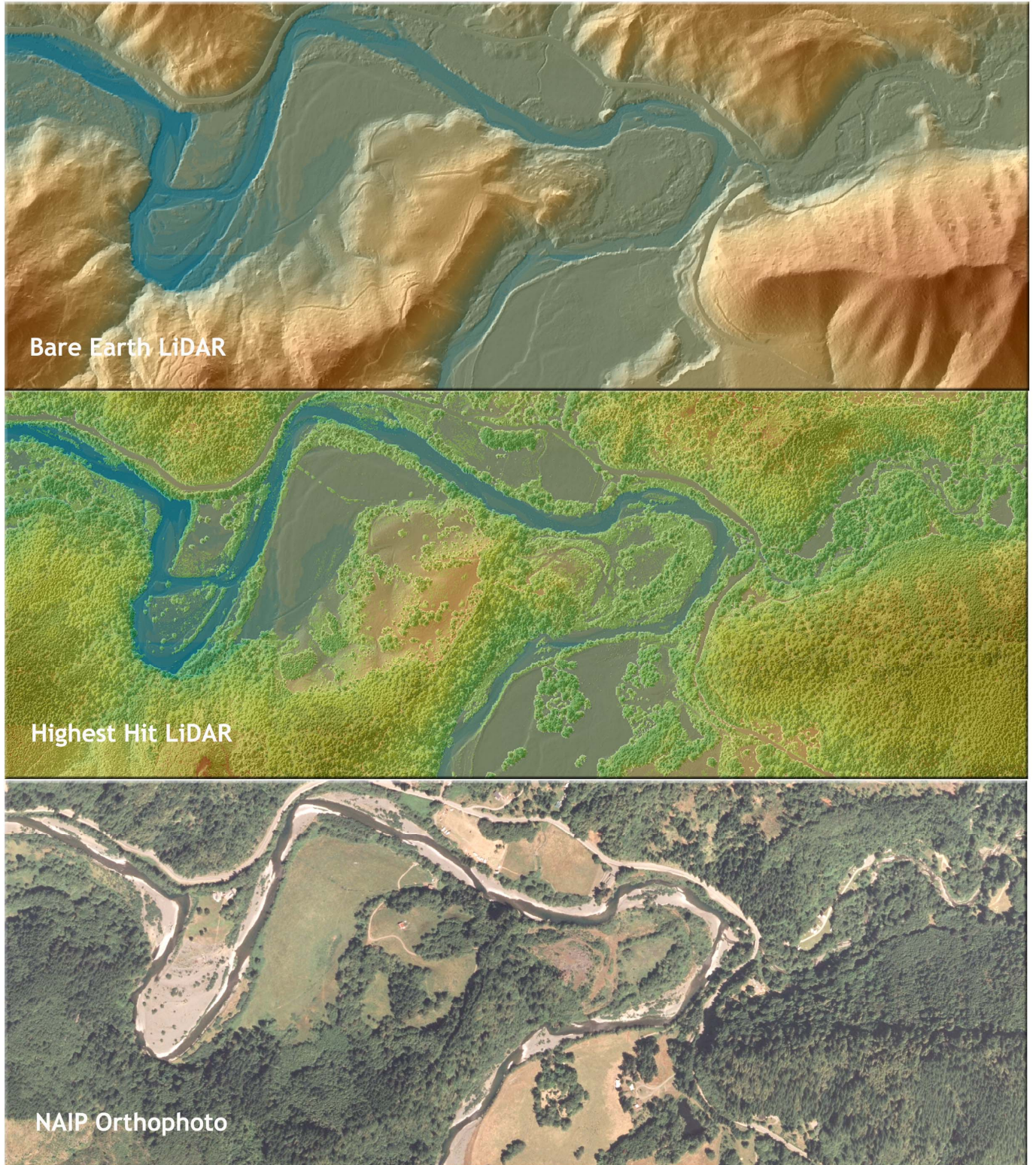


Figure 4.10. View of the confluence of Sixes River and Edson Creek in delivery tile 42124g4. Top image derived from bare earth LiDAR, center image from highest hit LiDAR, and lower image derived from NAIP orthophotos.



Figure 4.11. Stream confluence entering South Slough just north of Cox Canyon in delivery tile 43124C3. Upper image derived from highest hit LiDAR, center image derived from bare earth LiDAR, lower image derived from NAIP orthophoto.



Figure 4.12. Coast beach north of Cape Arago State Park in delivery tile 43124C4. Upper image derived from highest hit LiDAR, center image derived from bare earth LiDAR, lower image derived from NAIP orthophoto.

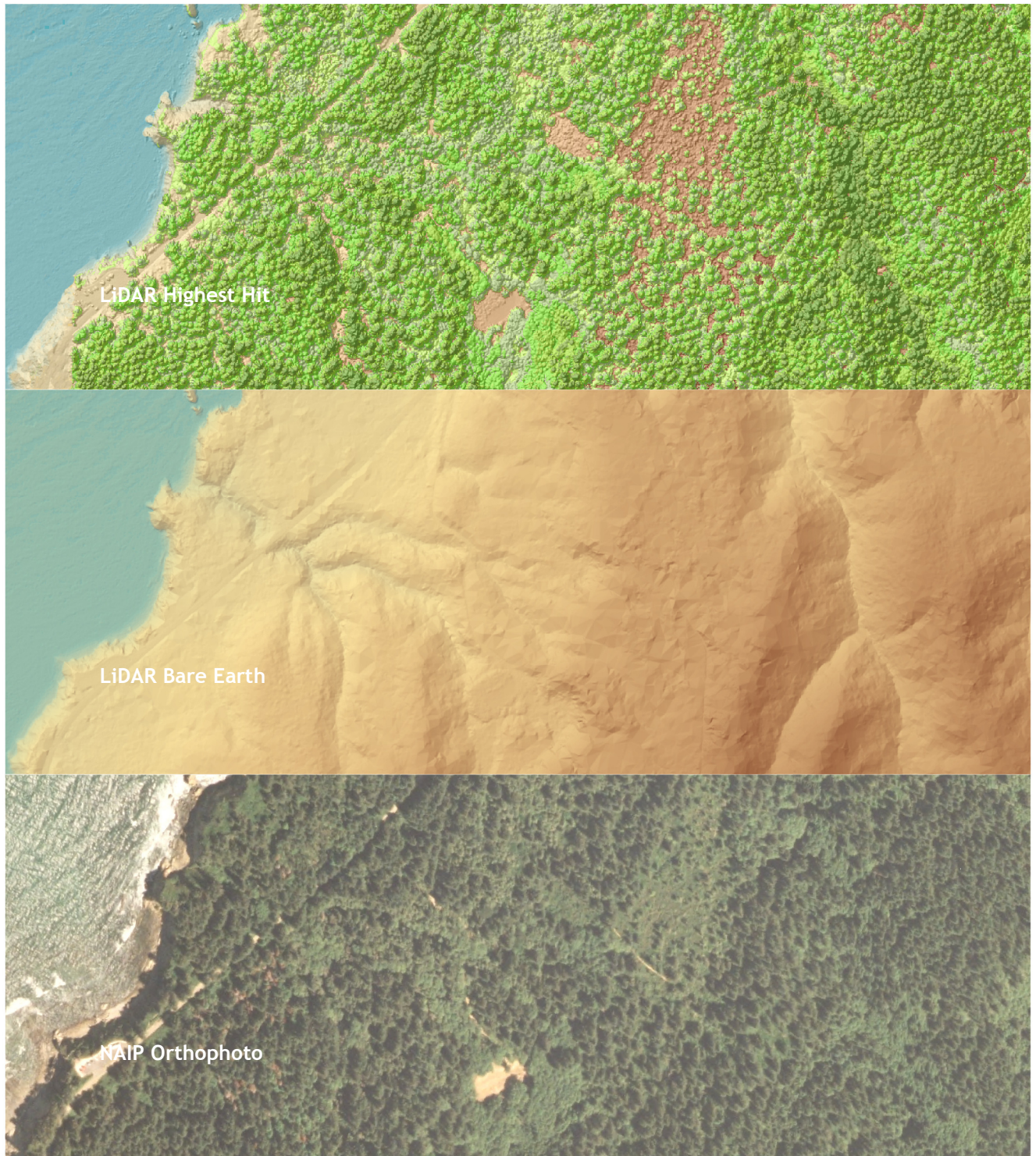


Figure 4.13. Upper Pony Creek Reservoir in delivery tile 43124C3. Upper image derived from highest hit LiDAR, center image derived from bare earth LiDAR, lower image derived from NAIP orthophoto.

